Table 3-1. Representative miRNAs That Were Commonly Repressed In CH-B, CH-C, HCC-B, and HCC-C Compared with Normal Liver (Cluster)

miRNA	Parametric *P* Value	Ratio*	No. of Significant Genes/Predicted Target Genes†	Hotelling Test *P* Value‡	Differentially Expressed Target Genes§	Pathway of Regulated Genes¶
hsa-miR-219	7.3E-05	0.28	25/109	2.59E-04	Glypican-3, ERP5, PLK2, HIRA, HMG2	Regulatory T cell differentiation
					ACOX1	Fatty acid beta-oxidation
					NF-X1	MHC class II biosynthetic process
hsa-miR-320	9.8E-05	0.50	26/88	3.50E-06	Vimentin, ALP (*N*-acetyltransferase-like), SEC61 beta, G-protein alpha-i2, Filamin A	Protein kinase cascade
					Rac1, RhoG	Organelle organization and biogenesis
					Vinexin beta, Profilin I, Ca-ATPase3	Actin cytoskeleton organization and biogenesis
hsa-miR-154	2.7E-04	0.15	22/70	5.40E-06	OTR, NET1(TSPAN1), NAP1, Vimentin, PDIA3, cytochrome P-450 reductase	Regulation of apoptosis
					DLX2	Morphogenesis
					GUAC, ACAT1	Branched chain family amino acid catabolic process
hsa-miR-29c	1.8E-03	0.55	53/133	1.00E-06	FBXO7, ASPP1, HSPA4, Cathepsin O, PDF, COL4A1, HSPA4, TIP30, CXADR	Cell-substrate adhesion
					NS1-BP, ALP (*N*-acetyltransferase-like), ACTR10, Beclin 1	Transcription, DNA-dependent
					SMAD6, LTBR(TNFRSF3), ENPP7	Apoptosis
hsa-miR-338	5.2E-03	0.46	30/101	3.60E-06	ID3, GATA-4, NFIA, FR-beta, CREST, HYOU1	Developmental process
					G3ST1, CAD,	Immune effector process
					FKBP12, LZIP, PDIA3, Schwannomin (NF2), CREST	Immune system process
hsa-miR-26a	6.3E-03	0.70	37/119	2.64E-05	*LIG4*, c-FLIP, GADD45 beta, DAPK1, PRDX4, LRP130	Response to stimulus
					Cyclin E, ZDHHC6, Tx1, ATG8 (GATE-16), WASP, C1s	DNA replication initiation
					COPG1	Ion transport
hsa-miR-126	8.1E-03	0.65	27/101	4.04E-03	ANP32B (april), HSPA4, RLI, LIV-1 (SLC39A6), PTP-MEG2, CD97, DHPR	Regulation of cellular protein metabolic process
					NFKBIA, NMI, MDH1, PDCD2	Response to stress
					SMAD6, ATP6AP2, ANP32B (april), NMI, HSPA4	Apoptosis
hsa-miR-325	8.7E-03	0.20	18/63	2.03E-04	TRADD, CREST, NEDD8, annexin IV, GPX2, PDF, TNFAIP1	Developmental process
					Glypican-3, ID1, PC-TP,	Multicellular organismal development
					SNRPB (Sm-B)	RNA splicing

*Ratio of HCC-B, HCC-C, CH-B, and CH-C to normal.
†The number of significant genes ($P < 0.05$) out of predicted target genes in which expression was evaluated in microarray.
‡Statistical assessment of presence of differentially expressed genes out of predicted target genes of miRNAs.
§Representative differentially expressed genes out of predicted target genes of miRNAs.
¶Representative pathway of differentially expressed genes out of predicted target genes of miRNAs.

the hypergeometrical distribution based on gene ontology terms. Because one gene is frequently involved in multiple pathways, all pathways corresponding to the genes with significance probability were listed.

Verification of Regulation of Candidate Target Genes by miRNAs. Anti-miRNA (Ambion) specific to 13 miRNAs (has-miR-17*, has-miR-20a, has-miR-23a, has-miR-26a, has-miR-27a, has-miR-29c, has-miR-30a, has-miR-92, has-miR-126, has-miR-139, has-miR-187, has-miR-200a, and has-miR-223) showing significant differences in expression were transfected into Huh7 cells using TransMessenger transfection reagent (QIAGEN, Valencia, CA), and loss of function of each miRNA was evaluated. Similarly, precursor miRNAs of five miRNAs (has-miR-23a, has-miR-26a, has-miR-27a, has-miR-92, and has-miR-200a) were also transfected into Huh7 cells, and gain of function of each miRNA was evaluated. The loss- and gain-of-function of miRNAs were evaluated via RTD-PCR. In addition, different gene expressions regulated by miRNAs were also evaluated via RTD-PCR.

HBV/HCV Infection Model Using Cultured Cells. The plasmid pHBV 1.2 coding the 1.2-fold length of the HBV genome was transfected into Huh7.5 cells using Fugene6 transfection reagent (Roche Applied Science, Indianapolis, IN). HBeAg production in culture medium was measured using Immunis HBeAg/Ab EIA (Institute of Immunology Co., Ltd., Tokyo, Japan).[13] The amount of HBV-DNA was measured via RTD-PCR (Supplementary Fig. 1A,B). JFH1-RNA was transfected into Huh7.5 cells using TransMessenger transfection reagent (QIAGEN) and the expression of the core protein was examined via immunofluorescence staining using anti-HCV core antibody (Affinity BioReagent, CO).[14,15] HCV-RNA amount was also measured via RTD-PCR (Supplementary Fig. 1A,B). JFH1/GND was used as a negative control. miRNA expression was quantitated by RTD-PCR 48 hours after transfection.

Results

Expression of miRNA in Liver Tissue. A panel of miRNA was successfully amplified from liver tissues via RTD-PCR. The representative amplification profile of miRNA as determined with RTD-PCR is shown in Fig. 1. To assess the reliability and reproducibility of this assay system, we first measured RNU6B in duplicate from all samples in different plates. The mean difference in Ct values of RNU6B expression within the same samples was 0.08 ± 0.05 (mean $\pm$ standard deviation), indicating the high reproducibility of this assay. All Ct values from each reaction were collected, and Ct variation obtained by each probe from all patients was calculated. Although RNU6B was frequently used as the internal control, the standard Ct variation was relatively high (Ct, 27 ± 1.94), suggesting that the variances in its value depend on the state of liver disease (N, CH and HCC). Therefore, we selected has-miR-328 as the internal control with the smallest standard deviation (Ct, 30 ± 0.60). The relative expression ratio of individual miRNA to has-miR-328 was calculated and applied to the following analysis using a BRB-array tool.

Hierarchical cluster analysis revealed that the expression profiles of the 188 miRNAs from each patient were roughly classified into normal liver, HBV-infected liver (CH-B+HCC-B; HBV group), and HCV-infected liver (CH-C+HCC-C; HCV group) (Fig. 2A). HCV viremia in two patients with CH-C was persistently cleared by interferon therapy before HCC development. The background liver of one of these patients was clustered in the normal group and those of others in the HCV group. Although these two patients were not clearly differentiated from others, some miRNAs such as miR-194, miR-211, and miR-340 that were down-regulated in the HCV group were significantly up-regulated in two patients (Fig. 3, cluster 2).

The present CH and HCC expression data were obtained from the same patient; however, each sample clustered irrespective of pairs in all but two patients. miRNA expression profiling was therefore more dependent on the disease condition than on the paired condition, as also confirmed by the Dunnett test.[12] We then attempted to classify the expression profiles into HBV and HCV groups using supervised learning methods (Table 2-1). HBV and HCV groups were significantly differentiated at an 87% accuracy ($P < 0.001$). The normal liver and CH (CH-B + CH-C) and CH and HCC (HCC-B + HCC-C) were also significantly differentiated at a 90% rate of accuracy. These results suggest that different stages of liver disease (normal, CH, and HCC) can be differentiated from each other based on the miRNA expression profile, as well as HBV and HCV infection.

To examine the relationship among five categories of groups, namely, N, CH-B, CH-C, HCC-B and HCC-C, we attempted to differentiate the five groups using a supervised learning algorithm (binary tree classification) used for classifying three or more groups. SVM was used as a prediction method. Expression profiles were first classified into groups N (normal) and non-N (non-normal) (CH-C, CH-B, HCC-C, and HCC-B) (node 1) ($P < 0.01$). The non-N group was then classified into HBV and HCV (node 2) ($P < 0.01$). The HBV group was further classified into CH-B and HCC-B (node 3) ($P < 0.01$), and the HCV group was further classified into CH-C and HCC-C (node 4) ($P < 0.01$) (Fig. 2B, Table 2-2). Thus, the findings support the notion that differences in miRNA expression between HBV and HCV are as distinct as those between CH and HCC.

Out of 20 miRNAs that differentiated node 1 classification (Table 2-2), 12 also differentiated node 3 or node 4 classification. The remaining eight miRNAs specifically differentiated node 1 classification. They were down-regulated in the HBV and HCV groups compared with the normal group (Fig. 3, cluster 1). Nineteen miRNAs differentiated node 2 classification (Table 2-2) and the hierarchical clustering using these miRNAs clearly differentiated the HBV and HCV groups (Fig. 3, cluster 2). There were 15 and 14 miRNAs that differentiated node 3 and 4 classifications, respectively (Table 2-2). Hierarchical clustering using these miRNAs revealed that these miRNAs differentiated CH-B and HCC-B as well as CH-C and HCC-C, respectively; 17 miRNAs were down-regulated in HCC, and six were up-regulated in HCC (Fig. 3, cluster 3).

Table 3-2. Differentially Expessed miRNA Between HCC-B, CH-B, and HCC-C, CH-C, and Their Representative Target Genes (Cluster 2)

miRNA	Parametric *P* Value	Ratio*	No. of Significant Genes/Predicted Target Genes†	Hotelling Test *P* Value‡	Differentially Expressed Target Genes§	Pathway of Regulated Genes¶
hsa-miR-190	1.2E-05	2.06	21/68	4.47E-02	Chk1, C2orf25, VRK2, USP16, STAF65(gamma)	Regulation of cell cycle
					AP1S2, RNASE4	Mitotic cell cycle
					PPP2R1B, ARHGAP15, UBPY	Negative regulation of apoptosis
hsa-miR-134	2.3E-04	5.74	11/58	3.40E-06	VKDGC, SH2B, MALS-1, DDB2	Multicellular organismal process
					BCRP1	Regulation of viral reproduction
					DDB2	Lipid biosynthetic process
hsa-miR-151	2.8E-04	1.82	12/62	6.41E-01	RGS2, UFO, AK2, USP7	G-protein signaling
					eIF4G2, USP7	Regulation of translation
					SLC22A7	Organic anion transport
hsa-miR-193	5.0E-04	1.67	23/95	9.30E-01	G-protein alpha-11, p130CAS, VAV-1, PDCD11	Cell motility
					Colipase, ACSA	Energy coupled proton transport
					DCOR	Intracellular signaling cascade
hsa-miR-133b	1.7E-03	2.42	20/97	3.69E-02	DDB2, Bcl-3, Cystatin B	Proteasomal protein catabolic process
					Rab-3, RAG1AP1, KCNH2, DCOR	Regulation of biological quality
					AL1B1	Carbohydrate metabolic process
hsa-miR-324-5p	2.9E-03	1.51	27/121	1.90E-06	SKAP55, VAV-1, DDB2, E2A, NIP1	Cellular developmental process
					MEMO (CGI-27), Rab-3	Cellular structure morphogenesis
					COPG1, GPX3, OAZ2	Glutathione metabolic process
hsa-miR-182*	3.1E-03	2.23	28/123	< 1e-07	Alpha-endosulfine, HCCR-2, Thioredoxin-like 2, TPT1, USP7	Translation initiation in response to stress
					DDB2, TPT1	Cellular developmental process
					JIP-1	JNK cascade
hsa-miR-105	4.6E-03	4.38	18/68	4.74E-05	Beta-2-microglobulin, HLA-B27	Antigen processing and presentation
					PIMT, IL-17RC	Immune response
					MHC class I, CDK9, ERG1, Desmocollin 3	
hsa-miR-211	5.3E-03	25.61	10/56	2.00E-04	PSMD5, SLC26A6	Proteasomal protein catabolic process
hsa-miR-20	5.7E-03	1.52	27/113	5.28E-03	Noelin, SC4MOL, Thioredoxin-like 2, CCL5, NALP3	Regulation of apoptosis
					Hic-5/ARA55, USP16, MAP4, Ferroportin 1	Positive regulation of cellular process
					TOP3A, PLRP1	Oxygen transport
hsa-miR-191	6.7E-03	1.39	25/79	7.55E-04	CDK9, GPS2, CLTA, LXR-alpha	Nucleic acid metabolic process
					ACSA	Acetyl-CoA biosynthetic process
					UGCGL1, SGPP1	Metal ion transport
hsa-miR-340	8.5E-03	1.48	17/81	3.73E-03	FKBP12, DCOR,	Calcium ion transport
					Gelsolin, VAV-1, ARF6	Actin cytoskeleton organization and biogenesis
					HXK3	Glucose catabolic process
hsa-miR-194	8.7E-03	1.67	13/74	5.90E-01	Cyclin B1, Serglycin	M phase of mitotic cell cycle
					PTE2	Acyl-CoA metabolic process
					SLC7A6	Carbohydrate utilization
hsa-miR-23a	1.9E-04	0.46	14/97	< 1e-07	*RGL2*, MANR, MEK1 (MAP2K1), Caspase-3, AZGP1	Protein kinase cascade
					FRK, Pyk2(FAK2), CSE1L	Cellular developmental process
					AZGP1	Defense response
hsa-miR-142-5p	4.9E-04	0.40	25/89	9.10E-06	Sirtuin4, PAI2, PSAT, RIL, CDC34, SPRY1	Metabotropic glutamate receptor
					E4BP4, DNAJC12, WWP1, PAIP1, PASK, rBAT	Regulation of gene expression
					VCAM1, CaMK I, WWP1, FHL3	Cell-matrix adhesion
hsa-miR-34c	5.1E-04	0.20	31/129	7.30E-06	Diacylglycerol kinase, zeta, PLC-delta 1, ATP2C1, PAI2	Manganese ion transport
					MLK3(MAP3K11), MEK1(MAP2K1), CDC25C, MRF-1, XPC	Protein kinase cascade
					GNT-IV	Inflammatory cell apoptosis

Table 3-2. Continued

miRNA	Parametric *P* Value	Ratio*	No. of Significant Genes/Predicted Target Genes†	Hotelling Test *P* Value‡	Differentially Expressed Target Genes§	Pathway of Regulated Genes¶
hsa-miR-124b	8.6E-04	0.32	25/120	7.10E-05	E2F5, Rad51, Jagged1	Muscle development
					MLK3(MAP3K11), RGS1	Intracellular signaling cascade
					COL16A1	MAPKKK cascade
hsa-let-7a	1.0E-03	0.45	28/136	9.35E-04	RAD51C, CoAA, hASH1, Cockayne syndrome B, Caspase-1, PP5	Response to DNA damage stimulus
					PLC-delta 1, MANR, ACADVL	Fibroblast proliferation
					HGF, NGF	Cellular developmental process
hsa-miR-27a	3.9E-03	0.59	18/108	1.19E-02	COL16A1, RIL, RhoGDI gamma, ANP32B (april)	Cytoskeleton organization and biogenesis
					VE-cadherin, NTH1, GATA-2, E4BP4	Response to external stimulus
					RAD51C	DNA recombination

*Ratio of HCC-B, CH-B, to HCC-C,CH-C.
†The number of significant genes ($p < 0.05$) out of predicted target genes in which expression was evaluated in microarray.
‡Statistical assesment of presence of differentially expressed genes out of predicted target genes of miRNAs.
§Representative differentially expressed genes out of predicted target genes of miRNAs.
¶Representative pathway of differentially expressed genes out of predicted target genes of miRNAs.

These results indicate that there were two types of miRNAs—one associated with HBV and HCV infection (cluster 2), the other associated with the stages of liver disease (clusters 1 and 2) that were irrelevant to the differences in HBV and HCV infection.

Differential miRNAs and Their Candidate Target Genes and Signaling Pathways. Differentially expressed miRNAs are shown in Table 3. In addition to the expression ratios of miRNAs in each group, the number of genes analyzed on the microarray predicted to be the target genes of miRNAs and that which actually showed significant ($P < 0.05$) differences in expression are also shown. Based on the frequencies and levels of expression of differential genes, the significance of regulation of these gene groups by miRNAs was evaluated using Hotelling T2 test (BRB ArrayTools) (Table 3). The representative candidate target genes and their signaling pathways by each miRNA were shown one by one (Table 3). The signaling pathways regulated by all differential miRNAs in each category of groups are shown in Table 4.

Eight miRNAs were down-regulated in the HBV and HCV groups compared with the normal group (Table 3-1; Fig. 3, cluster 1). These miRNAs were associated with an increased expression of genes related to cell adhesion, cell cycle, protein folding, and apoptosis (Tables 3-1, 4-1), and possibly with the common feature of CH irrespective of the differences in HBV and HCV infection.

Nineteen miRNAs clearly differentiated the HBV and HCV groups (Fig. 3, cluster 2, Table 3-2). Thirteen miRNAs exhibited a decreased expression in the HCV group, and six showed a decreased expression in the HBV group. miRNAs exhibiting a decreased expression in the HCV group regulate genes related to immune response, antigen presentation, cell cycle, proteasome, and lipid metabolism. On the other hand, those exhibiting a decreased expression in the HBV group regulate genes related to cell death, DNA damage and recombination, and transcription signals. These findings reflected the differences in the gene expression profile between CH-B and CH-C described (Tables 3-2, 4-2).[10] Interestingly, although these miRNAs were HBV and HCV infection–specific, some of them were reported to be tumor-associated miRNAs, suggesting the possible involvement of infection-associated miRNAs in HCC development.

Twenty-three miRNAs clearly differentiated CH and HCC that were irrelevant to the differences in HBV and HCV infection. Seventeen miRNAs were down-regulated in HCC that up-regulated cancer-associated pathways such as cell cycle, adhesion, proteolysis, transcription, translation, and the Wnt signaling pathway (Tables 3-3, 4-3). Six miRNAs were up-regulated in HCC that down-regulated all inflammation-mediated signaling pathways, potentially reflecting impaired antitumor immune response.

Relationship Between Expressions of Infection-Associated miRNA in Liver and Cultured Cells Infected with HBV and HCV. To clarify whether the expression of infection-associated miRNA is regulated by HBV and HCV infection, we investigated the relationship between changes in miRNA in liver tissues and those in miRNA in Huh7.5 cells in which infectious HBV or HCV clones replicated. To evaluate the replication of each clones in Huh7.5 cells, we measured time-course changes in the amounts of HBV-DNA and HCV-RNA in Huh7.5 cells transfected with pHBV1.2 and JFH1-RNA, respectively, by RTD-PCR (Supplementary Fig. 1A). The expression of HBV proteins was examined by measuring the amount

Table 3-3. Differentially Expessed miRNA Between CH and HCC and Their Representative Target Genes (Cluster 3)

miRNA	Parametric p-value	Ratio*	No. of Significant Genes/Predicted Target Genes†	Hotelling Test *P* Value‡	Differentially Expressed Target Genes§	Pathway of Regulated Genes¶
hsa-miR-139	4.50E-06	0.42	19/106	2.70E-03	Cyclin B1, DHX15, MCM5, Histone H2A	Mitotic cell cycle
					RBCK1, SYHH	Protein catabolic process
					ILK, IGFBP7, SAFB, CTR9	Response to external stimulus
hsa-miR-30a-3p	2.50E-05	0.49	26/144	1.73E-02	GGH, Pirin, ZNF207, Annexin VII	Regulation of oxidoreductase activity
					ILK, LTA4H, ABC50, GNPAT	Cell-matrix adhesion
					DLC1	Morphogenesis
hsa-miR-130a	7.00E-05	0.50	22/108	1.07E-02	SPHM, PPP2R5D, RHEB2, SPHM	Mitotic cell cycle
					MLK3(MAP3K11), Otubain1, TIMP4	Protein modification process
					NRBP	Cell differentiation
hsa-miR-223	3.40E-04	0.39	14/90	6.52E-03	Ephrin-A1, Midkine, FDPS	Cell morphogenesis
					K(+) channel, subfamily J	Notch signaling pathway
hsa-miR-187	3.55E-04	0.12	16/66	6.76E-04	HFE2, Otubain1	Negative regulation of programmed cell death
					PRSS11, SUPT5H, RAG1AP1	Developmental process
					PLOD3	Mitochondrial ornithine transport
hsa-miR-200a	6.86E-04	0.18	20/141	2.15E-02	*CDC25B, KAP3, CDK2AP2,* CHKA	Cell communication
					POLD	DNA replication
					CPSF4	RNA splicing
hsa-miR-17-3p	8.42E-04	0.58	28/108	8.98E-04	MLK3(MAP3K11), Tip60, ACBD6, DOC-1R, DAX1, RBCK1	Protein kinase cascade
					WNT5A, 14-3-3 gamma, DHX15	BMP signaling pathway
					HFE2, MCM5	DNA recombination
hsa-miR-99a	1.17E-03	0.53	33/163	9.52E-03	Calpain small subunit, Thoredoxin-like 2, Survivin	Cytokinesis
					IBP2, DNA-PK, KAP3,	Intracellular signaling cascade
					NFE2L1, PARP-1, HDAC11	Regulatory T cell differentiation
hsa-miR-200b	1.57E-03	0.18	24/147	2.72E-02	HSP47, HMG2, NRBP	Regulation of cell cycle
					SNX17	Cell motility
					Ephrin-A1	Receptor protein signaling pathway
hsa-miR-125b	1.82E-03	0.55	26/114	1.03E-01	COL4A2, TIP30, HSP47, MSP58	Cell adhesion
					MLK3(MAP3K11), ERK2 (MAPK1), ERK1 (MAPK3), PLOD3	Nuclear translocation of MAPK
					Otubain1, SCN4A(SkM1)	Ubiquitin-dependent protein catabolic process
hsa-miR-30e	2.10E-03	0.65	24/151	4.30E-02	Cyclin B1, XTP3B, GAK, Annexin VII, MIC2, NRBP	Mitotic cell cycle
					MSS4	Protein localization
					S100A10	Calcium ion transport
hsa-miR-199a*	4.26E-03	0.35	11/71	7.16E-02	BUB3, Cyclin B1, LMNBR	Mitotic cell cycle
					PRAME	Cardiac muscle cell differentiation
hsa-miR-122a	6.31E-03	0.51	11/80	1.01E-03	JAB1, APEX, Clathrin heavy chain	Base-excision repair
					PARN	Translational initiation
					DDAH2	Regulation of cellular respiration
hsa-miR-199a	8.77E-03	0.35	18/94	3.56E-02	IL-13, MLK3(MAP3K11), CLK2, ACP33	Protein amino acid phosphorylation
					PAFAH beta, SPA1, CLCN4	Small GTPase mediated signal transduction
hsa-miR-326	9.00E-03	0.57	29/147	2.25E-01	Midkine, ENT1, IP3KA, PSMC5, ANCO-1	Regulation of programmed cell death
					Thy-1, MCM6, Tip60, VILIP3	Cell-matrix adhesion
					COMP, Cathepsin A	Blood vessel development
hsa-miR-92	9.60E-03	0.81	28/140	2.47E-02	*TUBGCP2,* Fibrillin 1, PIPKI gamma, KAP3	Rho protein signal transduction
					SNX15, BCAT2	LDL receptor and BCAA metabolism
					IGFBP7, FZD6, COPS6	Adenosine receptor signaling pathway
hsa-miR-221	3.40E-06	3.34	16/67	3.59E-01	Lck, Kallistatin, Neuromodulin, LFA-3, PA24A, AZGP1, MSH2	Immune response-activating signal transduction
					KYNU, PMCA3	DNA repair

Table 3-3. *Continued*

miRNA	Parametric p-value	Ratio*	No. of Significant Genes/Predicted Target Genes†	Hotelling Test *P* Value‡	Differentially Expressed Target Genes§	Pathway of Regulated Genes¶
hsa-miR-222	6.50E-06	2.23	18/85	1.59E-02	Thrombospondin 1, Lck, MSH2, ATF-2, CITED2, Kallistatin	Cell motility
					PGAR	Triacylglycerol metabolic process
					KYNU	DNA replication
hsa-miR-301	5.22E-05	1.96	14/71	1.16E-01	Beta-2-microglobulin, PPCKM, PRC, Fra-1, PPCKM, ACAT2	Antigen processing and presentation
					BMPR1B, ARMER, EHM2, RBBP8	Meiotic recombination
					Neuromodulin, LDLR	Cell motility
hsa-miR-21	7.67E-03	1.57	19/81	1.86E-04	Btk, Fra-1, MSH2, Collectrin, Adipophilin	Regulation of T cell proliferation
					RNASE4, AGXT2L1	Peptidyl-tyrosine phosphorylation
					SARDH	Natural killer cell activation during immune response
hsa-miR-183	2.46E-02	3.51	13/86	3.36E-01	Hdj-2, PEMT, Lck, MKP-5, Chondromodulin-I, ABCA8	Cell differentiation
					IL-16, MTRR, SerRS	Methionine biosynthetic process
hsa-miR-98	5.22E-02	1.32	24/130	2.95E-04	ACAA2, LTB4DH, ACADVL, DECR, S14 protein,	Fatty acid metabolic process
					Rapsyn, Kallistatin, ENPEP, Beta crystallin B1	Multicellular organismal process
					CYP4F8	Prostaglandin metabolic process

*Ratio of HCC to CH.
†The number of significant genes ($P<0.05$) out of predicted target genes in which expression was evaluated in microarray.
‡Statistical assesment of presence of differentially expressed genes out of predicted target genes of miRNAs.
§Representative differentially expressed genes out of predicted target genes of miRNAs.
¶Representative pathway of differentially expressed genes out of predicted target genes of miRNAs.

of HBeAg released in culture medium (Supplementary Fig. 1B). HCV protein expression was examined by evaluating the core protein expression after 48 hours by fluorescence immunostaining (Supplementary Fig. 1C). RNA was extracted from the Huh7.5 cells 48 hours after gene transfection, and miRNA expression pattern in the cells was compared with those in liver tissues. We found a strong correlation between differences in miRNA expression between liver tissues of the HBV and HCV groups, and those in miRNA expression between Huh7.5 cells transfected with HBV and HCV clones ($r = 0.73$, $P = 0.0006$) (Fig. 5). These results revealed that differences in the expression of infection-associated miRNA in the liver between the HBV and HCV groups are explained by changes in miRNA expression caused by HBV and HCV infections.

Verification of Regulation of Candidate Target Genes by miRNA. Anti-miRNAs (Ambion) specific to 13 miRNAs (has-miR-17*, has-miR-20a, has-miR-23a, has-miR-26a, has-miR-27a, has-miR-29c, has-miR-30a, has-miR-92, has-miR-126, has-miR-139, has-miR-187, has-miR-200a, and has-miR-223) showing significant differences in expression were transfected into Huh7 cells to examine loss of function of the miRNAs. Five miRNAs (has-miR-23a, has-miR-26a, has-miR-27a, has-miR-92, and has-miR-200a) showed a decreased expression by more than 50%. Precursor miRNAs of these miRNAs were also transfected into the cells to examine the gain of function of the miRNAs (Supplementary Fig. 2). It was confirmed that the expressions of target genes of the five miRNAs (LIG4 [by has-miR-26a]; RGL2 [by has-miR-23a]; Rad51C [by has-miR-27a]; KAP3, CDC25B, KAP3, CDK2AP2, POLD, and CPSF4 [by has-miR-200a]; and TUBGCP2, SNX15 and BCAT2 [by has-miR-92]) were increased by the suppression of the miRNAs induced by anti-miRNAs and were decreased by the overexpression of precursor miRNAs (Supplementary Fig. 3).

Discussion

miRNA plays an important role in various diseases such as infection and cancer.[1-3] In this study, we examined miRNA expression profiles in normal liver and HCC, including nontumor lesions infected with HBV or HCV. Although the expression profiles of miRNAs in HCC have been reported,[16-18] most of the studies were performed using a microarray system. Because we thought that miRNAs could not produce enough detection signals owing to their short length, we applied a highly sensitive and quantitative RTD-PCR method for miRNAs. Moreover, global gene expression in the same tissues was ana-

Table 4-1. Pathway Analysis of Targeted Genes by miRNAs that Were Commonly Repressed in CH-B, CH-C, HCC-B, and HCC-C Compared with Normal Liver (Cluster 1)

No.	Pathway Name	P Value
Down-regulated miRNA in CH-B,HCC-B,CH-C and HCC-C (possibly up-regulating target genes)		
1	Cell adhesion_Platelet-endothelium-leukocyte interactions	1.11E-02
2	Cell cycle_S phase	2.18E-02
3	Protein folding_Protein folding nucleus	2.43E-02
4	Cell cycle_G1-S	3.07E-02
5	Development_Cartilage development	3.89E-02
6	Protein folding_Folding in normal condition	3.89E-02
7	Proteolysis_Connective tissue degradation	3.99E-02
8	Proteolysis_Proteolysis in cell cycle and apoptosis	4.31E-02
9	Signal Transduction_BMP and GDF signaling	5.81E-02
10	Immune_Antigen presentation	6.05E-02

lyzed via cDNA microarray to examine whether the differentially expressed miRNAs could regulate their target genes. Because the absolute standard of miRNA is not available at present, and miRNA expression was compared within the samples and genes analyzed in this study, there might be possible errors when a larger number of samples and genes were analyzed.

Using these systems, we found that the expression profile in miRNAs was clearly different according to HBV and HCV infection for the first time. The differences were confirmed by the nonsupervised learning method, hierarchical clustering (Fig. 2A), and supervised learning methods based on SVM at an 87% accuracy ($P < 0.001$) (Table 2-1). As similarly described, the expression profile in miRNAs was significantly different according to the progression of liver disease (normal, CH, and HCC) in this study. The present CH and HCC expression data were derived from the same patient, and some microarray analyses suggested that the noncancerous liver tissue can predict the prognosis of HCC.[19,20] We examined whether the miRNA expression of paired samples was similar or independent using the Dunnett test[12] (Supplementary Data). Our data indicated that miRNA expression profiling was more dependent on the disease condition than on the paired condition, although the issue of paired samples should be taken into account carefully.

Table 4-2. Pathway Analysis of Targeted Genes by Differentially Expressed miRNAs Between HBV-Related Liver Disease (CH-B,HCC-B) and HCV Related Liver Disease (CH-C,HCC-C Cluster 2)

No.	Pathway Name	P Value
Down-regulated miRNA in CH-C,HCC-C (possibly up-regulating target genes)		
1	Immune_Phagosome in antigen presentation	5.80E-04
2	Muscle contraction	1.05E-03
3	Immune_Antigen presentation	5.75E-03
4	Cell cycle_Meiosis	1.49E-02
5	Reproduction_Male sex differentiation	2.06E-02
6	Cell adhesion_Platelet aggregation	2.77E-02
7	Transport_Synaptic vesicle exocytosis	3.56E-02
8	Inflammation_Kallikrein-kinin system	3.73E-02
9	Inflammation_IgE signaling	4.10E-02
10	Development_Skeletal muscle development	5.02E-02
Down-regulated miRNA in CH-B,HCC-B (possibly up-regulating target genes)		
1	Signal Transduction_Cholecystokinin signaling	1.15E-04
2	Inflammation_NK cell cytotoxicity	5.29E-03
3	Signal transduction_CREM pathway	5.31E-03
4	Reproduction_GnRH signaling pathway	7.80E-03
5	DNA damage_DBS repair	1.02E-02
6	Cell cycle_G2-M	1.63E-02
7	Development_Neuromuscular junction	2.07E-02
8	Apoptosis_Apoptosis mediated by external signals	2.42E-02
9	Reproduction_FSH-beta signaling pathway	2.92E-02
10	Cell adhesion_Amyloid proteins	3.81E-02

Table 4-3. The Pathway Analysis of Targeted Genes by Differentially Expressed miRNAs Between CH and HCC (Cluster 3)

No.	Pathway Name	P Value
	Down-regulated miRNA in HCC (possibly up-regulating target genes)	
1	Cytoskeleton_Spindle microtubules	2.15E-03
2	Transcription_Chromatin modification	5.27E-03
3	Proteolysis_Ubiquitin-proteasomal proteolysis	6.43E-03
4	Cell adhesion_Cell-matrix interactions	7.30E-03
5	Cell cycle_Meiosis	7.83E-03
6	DNA damage_Checkpoint	1.69E-02
7	Reproduction_Progesterone signaling	1.94E-02
8	Apoptosis_Apoptotic mitochondria	3.14E-02
9	Translation_Regulation of initiation	4.22E-02
10	Signal transduction_WNT signaling	4.26E-02
	Up-regulated miRNA in HCC (possibly down-regulating target genes)	
1	Inflammation_IgE signaling	1.05E-02
2	Inflammation_Kallikrein-kinin system	2.46E-02
3	Inflammation_Innate inflammatory response	2.51E-02
4	Inflammation_Histamine signaling	4.25E-02
5	Inflammation_Neutrophil activation	4.55E-02
6	Chemotaxis	4.68E-02
7	Inflammation_IL-12,15,18 signaling	5.16E-02
8	Inflammation_NK cell cytotoxicity	7.25E-02
9	Cell cycle_G0-G1	7.53E-02
10	Inflammation_Complement system	7.72E-02

Binary tree prediction analysis and detailed assessment of hierarchical clustering revealed two types of differential miRNAs, one associated with HBV and HCV infection, the other associated with the stages of liver disease that were irrelevant to the differences in HBV and HCV infection. We found that differences in miRNA expression between liver tissues with HBV and HCV (HBV/HCV) were strongly correlated with those in miRNA between cultured cell models of HBV and HCV infection (HBV/HCV) ($r = 0.73$ $P = 0.0006$) (Fig. 5). Thus, there exist HBV- and HCV-infection–specific miRNAs that potentially regulate viral replication and host gene signaling pathways in hepatocytes.

	HBV/HCV	
	Tissue	Huh7.5
hsa-miR-20	0.61	0.36
hsa-miR-23a	-1.12	-1.3
hsa-miR-27a	-0.75	-1.51
hsa-miR-34c	-2.29	N.D.
hsa-miR-105	2.13	N.D.
hsa-miR-124b	-1.63	-10.54
hsa-miR-133b	1.28	-3.64
hsa-miR-134	2.52	-0.63
hsa-miR-142-5p	-1.34	-4.39
hsa-miR-151	0.86	-0.29
hsa-miR-182*	1.16	0.37
hsa-miR-190	1.04	1.32
hsa-miR-191	0.48	1.16
hsa-miR-193	0.74	-0.03
hsa-miR-194	0.74	0.76
hsa-miR-211	4.68	5.26
hsa-miR-324-5p	0.59	1.16
hsa-miR-340	0.57	1.68
hsa-let-7a	-1.14	-4.51

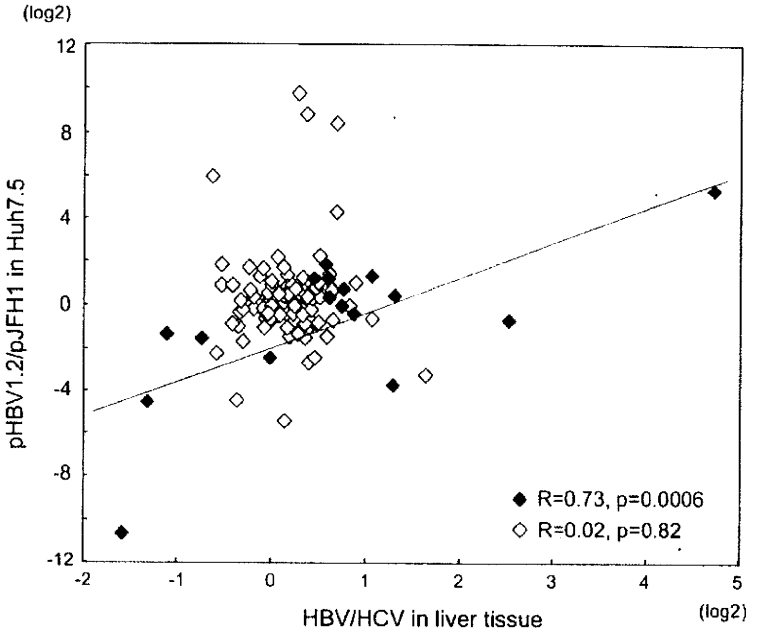

Fig. 5. Correlation between differences in miRNA expression between liver tissues infected with HBV and HCV and those in miRNA expression between cultured cell models of HBV and HCV infections. A total of 140 of 188 miRNAs were confirmed to be expressed in Huh7.5 cells. There was a significant correlation of infection-associated miRNA (closed lozenge) in vitro and in vivo ($r = 0.73$, $P = 0.0006$), but none for the other 121 miRNAs (open lozenge) ($r = 0.02$, $P = 0.82$).

The pathway analysis of targeted genes by miRNAs revealed that 13 miRNAs exhibiting a decreased expression in the HCV group regulate genes related to immune response, antigen presentation, cell cycle, proteasome, and lipid metabolism. Six miRNAs showing a decreased expression in the HBV group regulate genes related to cell death, DNA damage and recombination, and transcription signals. These findings reflected differences in the gene expression profile between CH-B and CH-C as described.[10] Many of the miRNAs were down-regulated in the HCV group rather than in the HBV group. It has been reported that human endogenous miRNAs may be involved in defense mechanisms, mainly against RNA viruses.[21] On the other hand, it is suggested that endogenous miRNAs may be consumed and reduced by defense mechanisms, especially those against RNA viruses.

Although the expressions of these HBV- and HCV-infection–specific miRNAs were irrelevant to the differences in CH and HCC (Fig. 3, cluster 2), some of them have been reported to play pivotal roles in the occurrence of cancer. For example, has-let-7a regulates ras and c-myc genes,[22] and has-miR-34 is involved in the p53 tumor suppressor pathway.[23] These miRNAs were down-regulated in the HBV group, possibly participating in a more aggressive and malignant phenotype in HCC-B rather than in HCC-C. High expression of has-miR-191 was shown to be significantly associated with the worse survival in acute myeloid leukemia,[24] and has-miR-191 was overexpressed in the HBV group compared with the HCV group. On the other hand, has-miR-133b, which was reported to be down-regulated in squamous cell carcinoma,[25] was repressed in the HCV group compared with the HBV group. Some hematopoietic-specific miRNAs such as has-miR-142-5p were up-regulated in the HCV group. Therefore, these miRNAs were not only HBV and HCV infection–associated but also tumor-associated. These findings indicate different mechanisms of development of HCC infected with HBV and HCV (Fig. 6).

Following HCC development, common changes in miRNA expression between HCC-B and HCC-C appeared (Fig. 3, cluster 3). The 23 miRNAs mentioned above clearly differentiated CH and HCC that were irrelevant to the differences in HBV and HCV infections. Seventeen miRNAs were down-regulated in HCC, which up-regulated cancer-associated pathways. Six miRNAs were up-regulated in HCC that down-regulated all inflammation-mediated signaling pathways, potentially reflecting impaired antitumor immune response in HCC. These results suggest that common signaling pathways are involved in HCC development from CH, and that HBV- and HCV-specific miRNAs participate in generating HCC-specific miRNA expressions (Fig. 6). Therefore, these miRNAs might be good candidates for molecular targeting to prevent HCC occurrence, because they reg-

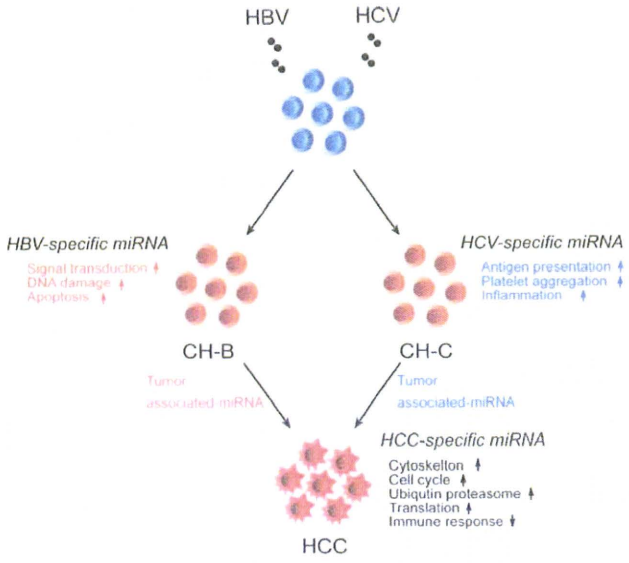

Fig. 6. Infection-associated and HCC-specific miRNAs and liver disease progression.

ulate a common signaling pathway underlying HCC-B and HCC-C development.

In conclusion, we showed that miRNAs are important mediators of HBV and HCV infections as well as liver disease progression. Further studies are needed to enable more detailed mechanistic analysis of the miRNAs identified here and to evaluate the usefulness of miRNAs as diagnostic/prognostic markers and potential therapeutic target molecules.

Acknowledgement: The authors thank Mikiko Nakamura and Nami Nishiyama for excellent technical assistance.

References

1. He L, Thomson JM, Hemann MT, Hernando-Monge E, Mu D, Goodson S, et al. A microRNA polycistron as a potential human oncogene. Nature 2005;435:828-833.
2. Calin GA, Dumitru CD, Shimizu M, Bichi R, Zupo S, Noch E, et al. Frequent deletions and down-regulation of micro-RNA genes miR15 and miR16 at 13q14 in chronic lymphocytic leukemia. Proc Natl Acad Sci U S A 2002;99:15524-15529.
3. Cho WC. OncomiRs: the discovery and progress of microRNAs in cancers. Mol Cancer 2007;6:60.
4. Hutvagner G, Zamore PD. A microRNA in a multiple-turnover RNAi enzyme complex. Science 2002;297:2056-2060.
5. Ambros V, Bartel B, Bartel DP, Burge CB, Carrington JC, Chen X, et al. A uniform system for microRNA annotation. RNA 2003;9:277-279.
6. Lee RC, Feinbaum RL, Ambros V. The C. elegans heterochronic gene lin-4 encodes small RNAs with antisense complementarity to lin-14. Cell 1993;75:843-854.
7. Lewis BP, Burge CB, Bartel DP. Conserved seed pairing, often flanked by adenosines, indicates that thousands of human genes are microRNA targets. Cell 2005;120:15-20.
8. Kiyosawa K, Sodeyama T, Tanaka E, Gibo Y, Yoshizawa K, Nakano Y, et al. Interrelationship of blood transfusion, non-A, non-B hepatitis and hepatocellular carcinoma: analysis by detection of antibody to hepatitis C virus. HEPATOLOGY 1990;12:671-675.
9. Honda M, Kaneko S, Kawai H, Shirota Y, Kobayashi K. Differential gene expression between chronic hepatitis B and C hepatic lesion. Gastroenterology 2001;120:955-966.
10. Honda M, Yamashita T, Ueda T, Takatori H, Nishino R, Kaneko S. Different signaling pathways in the livers of patients with chronic hepatitis B or chronic hepatitis C. HEPATOLOGY 2006;44:1122-1138.
11. Molinaro AM, Simon R, Pfeiffer RM. Prediction error estimation: a comparison of resampling methods. Bioinformatics 2005;21:3301-3307.
12. Dunnett CW. A multiple comparison procedure for comparing several treatments with a control. J Am Stat Assoc 1955;50:1096-1121.
13. Weiss L, Kekule AS, Jakubowski U, Burgelt E, Hofschneider PH. The HBV-producing cell line HepG2-4A5: a new in vitro system for studying the regulation of HBV replication and for screening anti-hepatitis B virus drugs. Virology 1996;216:214-218.
14. Lindenbach BD, Evans MJ, Syder AJ, Wolk B, Tellinghuisen TL, Liu CC, et al. Complete replication of hepatitis C virus in cell culture. Science 2005;309:623-626.
15. Wakita T, Pietschmann T, Kato T, Date T, Miyamoto M, Zhao Z, et al. Production of infectious hepatitis C virus in tissue culture from a cloned viral genome. Nat Med 2005;11:791-796.
16. Murakami Y, Yasuda T, Saigo K, Urashima T, Toyoda H, Okanoue T, et al. Comprehensive analysis of microRNA expression patterns in hepatocellular carcinoma and non-tumorous tissues. Oncogene 2006;25:2537-2545.
17. Varnholt H, Drebber U, Schulze F, Wedemeyer I, Schirmacher P, Dienes HP, et al. MicroRNA gene expression profile of hepatitis C virus-associated hepatocellular carcinoma. HEPATOLOGY 2008;47:1223-1232.
18. Budhu A, Jia HL, Forgues M, Liu CG, Goldstein D, Lam A, et al. Identification of metastasis-related microRNAs in hepatocellular carcinoma. HEPATOLOGY 2008;47:897-907.
19. Budhu A, Forgues M, Ye QH, Jia HL, He P, Zanetti KA, et al. Prediction of venous metastases, recurrence, and prognosis in hepatocellular carcinoma based on a unique immune response signature of the liver microenvironment. Cancer Cell 2006;10:99-111.
20. Hoshida Y, Villanueva A, Kobayashi M, Peix J, Chiang DY, Camargo A, et al. Gene expression in fixed tissues and outcome in hepatocellular carcinoma. N Engl J Med 2008;359:1995-2004.
21. Jopling CL, Yi M, Lancaster AM, Lemon SM, Sarnow P. Modulation of hepatitis C virus RNA abundance by a liver-specific MicroRNA. Science 2005;309:1577-1581.
22. Johnson CD, Esquela-Kerscher A, Stefani G, Byrom M, Kelnar K, Ovcharenko D, et al. The let-7 microRNA represses cell proliferation pathways in human cells. Cancer Res 2007;67:7713-7722.
23. He X, He L, Hannon GJ. The guardian's little helper: microRNAs in the p53 tumor suppressor network. Cancer Res 2007;67:11099-11101.
24. Garzon R, Volinia S, Liu CG, Fernandez-Cymering C, Palumbo T, Pichiorri F, et al. MicroRNA signatures associated with cytogenetics and prognosis in acute myeloid leukemia. Blood 2008;111:3183-3189.
25. Wong TS, Liu XB, Chung-Wai Ho A, Po-Wing Yuen A, Wai-Man Ng R, Ignace Wei W. Identification of pyruvate kinase type M2 as potential oncoprotein in squamous cell carcinoma of tongue through microRNA profiling. Int J Cancer 2008;123:251-257.

GASTROENTEROLOGY 2009;136:1012–1024

EpCAM-Positive Hepatocellular Carcinoma Cells Are Tumor-Initiating Cells With Stem/Progenitor Cell Features

TARO YAMASHITA,* JUNFANG JI,* ANURADHA BUDHU,* MARSHONNA FORGUES,* WEN YANG,‡ HONG-YANG WANG,‡ HULIANG JIA,§ QINGHAI YE,§ LUN-XIU QIN,§ ELAINE WAUTHIER,‖ LOLA M. REID,‖ HIROSHI MINATO,¶ MASAO HONDA,¶ SHUICHI KANEKO,¶ ZHAO-YOU TANG,§ and XIN WEI WANG*

*Liver Carcinogenesis Section, Laboratory of Human Carcinogenesis, Center for Cancer Research, National Cancer Institute, Bethesda, Maryland; ‡International Cooperation Laboratory on Signal Transduction, Eastern Hepatobiliary Surgery Institute, Shanghai, China; §Liver Cancer Institute and Zhongshan Hospital, Fudan University, Shanghai, China; ‖Department of Cell and Molecular Physiology, University of North Carolina School of Medicine, Chapel Hill, North Carolina; and the ¶Liver Disease Center and Kanazawa University Hospital, Kanazawa University, Kanazawa, Japan

Background & Aims: **Cancer progression/metastases and embryonic development share many properties including cellular plasticity, dynamic cell motility, and integral interaction with the microenvironment. We hypothesized that the heterogeneous nature of hepatocellular carcinoma (HCC), in part, may be owing to the presence of hepatic cancer cells with stem/progenitor features.** ***Methods:*** **Gene expression profiling and immunohistochemistry analyses were used to analyze 235 tumor specimens derived from 2 recently identified HCC subtypes ($EpCAM^+$ α-fetoprotein [AFP^+] HCC and $EpCAM^-$ AFP^- HCC). These subtypes differed in their expression of AFP, a molecule produced in the developing embryo, and EpCAM, a cell surface hepatic stem cell marker. Fluorescence-activated cell sorting was used to isolate $EpCAM^+$ HCC cells, which were tested for hepatic stem/progenitor cell properties.** ***Results:*** **Gene expression and pathway analyses revealed that the $EpCAM^+$ AFP^+ HCC subtype had features of hepatic stem/progenitor cells. Indeed, the fluorescence-activated cell sorting–isolated $EpCAM^+$ HCC cells displayed hepatic cancer stem cell–like traits including the abilities to self-renew and differentiate. Moreover, these cells were capable of initiating highly invasive HCC in nonobese diabetic, severe combined immunodeficient mice. Activation of Wnt/β-catenin signaling enriched the $EpCAM^+$ cell population, whereas RNA interference-based blockage of EpCAM, a Wnt/β-catenin signaling target, attenuated the activities of these cells.** ***Conclusions:*** **Taken together, our results suggest that HCC growth and invasiveness is dictated by a subset of $EpCAM^+$ cells, opening a new avenue for HCC cancer cell eradication by targeting Wnt/β-catenin signaling components such as EpCAM.**

Tumors originate from normal cells as a result of accumulated genetic/epigenetic changes. Although considered monoclonal in origin, tumor cells are heterogeneous in their morphology, clinical behavior, and molecular profiles.[1,2] Tumor cell heterogeneity has been explained previously by the clonal evolution model[3]; however, recent evidence has suggested that heterogeneity may be owing to derivation from endogenous stem/progenitor cells[4] or de-differentiation of a transformed cell.[5] This hypothesis supports an early proposal that cancers represent "blocked ontogeny"[6] and a derivative that cancers are transformed stem cells.[7] This renaissance of stem cells as targets of malignant transformation has led to realizations about the similarities between cancer cells and normal stem cells in their capacity to self-renew, produce heterogeneous progenies, and limitlessly divide.[8] The cancer stem cell (CSC) (or tumor-initiating cell) concept is that a subset of cancer cells bear stem cell features that are indispensable for a tumor. Accumulating evidence suggests the involvement of CSCs in the perpetuation of various cancers including leukemia, breast cancer, brain cancer, prostate cancer, and colon cancer.[9–13] Experimentally, putative CSCs have been isolated using cell surface markers specific for normal stem cells. Stem cell–like features of CSC have been confirmed by functional in vitro clonogenicity and in vivo tumorigenicity assays. For example, leukemia-initiating cells in nonobese diabetic, severe combined immunodeficient (NOD/SCID) mice are $CD34^{-+}CD38^-$.[11] Breast cancer CSCs are $CD44^+CD24^{-/low}$ cells, whereas tumor-initiating cells of the brain, colon, and prostate are $CD133^+$.[10,12,13] CSCs are considered more metastatic and drug-/radiation-resistant than non-CSCs in the tumor, and are responsible for cancer relapse. These findings warrant the development of treatment strategies that can specifically eradicate CSCs.[14,15]

Abbreviations used in this paper: AFP, α-fetoprotein; BIO, 6-bromoindirubin-3′-oxime; CSC, cancer stem cell; FACS, fluorescence-activated cell sorting; 5-FU, 5-fluorouracil; HpSC, hepatic stem cell; IF, immunofluorescence; IHC, immunohistochemistry; MACS, magnetic-activated cell sorting; MeBIO, 1-methyl-BIO; MH, mature hepatocyte; PCNA, proliferating cell nuclear antigen; siRNA, small interfering RNA.

0016-5085/09/$36.00
doi:10.1053/j.gastro.2008.12.004

Hepatocellular carcinoma (HCC) is the third leading cause of cancer death worldwide.[16] Although the cellular origin of HCC is unclear,[17,18] HCC has heterogeneous pathologies and genetic/genomic profiles,[19] suggesting that HCC can initiate in different cell lineages.[20] The liver is considered as a maturational lineage system similar to that in the bone marrow.[21] Experimental evidence indicates that certain forms of hepatic stem cells (HpSCs), present in human livers of all donor ages, are multipotent and can give rise to hepatoblasts,[22,23] which are, in turn, bipotent progenitor cells that can progress either into hepatocytic or biliary lineages.[22,24] α-fetoprotein (AFP) is one of the earliest markers detected in the liver bud specified from the ventral foregut,[25,26] but its expression has been found only in hepatoblasts and to a lesser extent in committed hepatocytic progenitors, not in later lineages or in normal human HpSC.[22] Recent studies also have indicated that EpCAM is a biomarker for HpSC because it is expressed in HpSCs and hepatoblasts.[22-24]

We recently identified a novel HCC classification system based on EpCAM and AFP status.[27] Gene expression profiles revealed that EpCAM$^+$ AFP$^+$ HCC (referred to as *HpSC-HCC*) has progenitor features with poor prognosis, whereas EpCAM$^-$ AFP$^-$ HCC (referred to as *mature hepatocyte-like HCC*; MH-HCC) have adult hepatocyte features with good prognosis. Wnt/β-catenin signaling, a critical player for maintaining embryonic stem cells,[28] is activated in EpCAM$^+$ AFP$^+$ HCC, and EpCAM is a direct transcriptional target of Wnt/β-catenin signaling.[29] Moreover, EpCAM$^+$ AFP$^+$ HCC cells are more sensitive to β-catenin inhibitors than EpCAM$^-$ HCC cells in vitro.[29] Interestingly, a heterogeneous expression of EpCAM and AFP was observed in clinical tissues, a feature that may be attributed to the presence of a subset of CSCs. In this study, we have confirmed that EpCAM$^+$ HCC cells are highly invasive and tumorigenic, and have activated Wnt/β-catenin signaling. We also show a crucial role of EpCAM in the maintenance of hepatic CSCs. Our data shed new light on the pathogenesis of HCC and may open new avenues for therapeutic interventions for targeting hepatic CSCs.

Materials and Methods

Clinical Specimens

HCC samples were obtained with informed consent from patients who underwent radical resection at the Liver Cancer Institute of Fudan University, Eastern Hepatobiliary Surgery Institute, and the Liver Disease Center of Kanazawa University Hospital, and the study was approved by the institutional review boards of the respective institutes. The microarray data from clinical specimens are available publicly (GEO accession number, GSE5975).[27] Array data from a total of 156 HCC cases (155 hepatitis B virus [HBV]-positive) corresponding to 2 subtypes of HCC (ie, HpSC-HCC and MH-HCC), were used to search for HpSC-HCC–associated genes (Supplementary Table 1; see supplementary material online at www.gastrojournal.org). A total of 79 formalin-fixed and paraffin-embedded HCC samples were used for immunohistochemistry (IHC) analyses (Supplementary Table 2; see supplementary material online at www.gastrojournal.org), 56 of which also were used in a recent study.[30] The classification of HpSC-HCC and MH-HCC was based on previously described criteria.[27]

Cell Cultures and Sorting

Human liver cancer cell lines (HuH1 and HuH7) were derived from Health Science Research Resources Bank (JCRB0199 and JCRB0403, respectively) and routinely cultured as previously described.[31] Normal human MHs, provided by the University of Pittsburgh through Liver Tissue Cell Distribution System, were cultured as previously described.[32] Human HpSCs were isolated from fetal livers and cultured in Kubota and Reid's[33] medium as previously described. Wnt10B conditioned medium was prepared as described.[34] Embryonic stem cell culture medium was prepared using Knockout Dulbecco's modified Eagle medium supplemented with 18% of Serum Replacement (Invitrogen, Carlsbad, CA). The pTOP-FLASH and pFOP-FLASH luciferase constructs were described previously.[29] BIO and MeBIO were generous gifts from Ali Brivanlou (The Rockefeller University, New York, NY). For isolating single cell–derived colonies to determine whether heterogeneity is an intrinsic property of EpCAM$^+$ cells, HuH1 and HuH7 cells were resuspended and plated as a single cell per well in 96-well plates. A total of 192 single cells were plated successfully. The clones that grew well were selected 2 weeks after seeding and used for immunofluorescence (IF) analysis. The 5-fluorouracil (5-FU) stock (2 mg/mL; Sigma, St Louis, MO), was prepared in distilled water. Fluorescence-activated cell sorting (FACS) and magnetic-activated cell sorting (MACS) analyses were used to isolate EpCAM$^+$ HCC cells (Supplementary materials; see supplementary Materials and Methods online at www.gastrojournal.org).

Clonogenicity, Spheroid Formation, Invasion, Quantitative Reverse Transcription–Polymerase Chain Reaction, and IHC Assays

For colony formation assays, 2000 EpCAM$^+$ or EpCAM$^-$ cells were seeded in 6-well plates after FACS. After 10 days of culture, cells were fixed by 100% methanol and stained with methylene blue. For spheroid assays, single-cell suspensions of 1000 EpCAM$^+$ or EpCAM$^-$ cells were seeded in 6-well Ultra-Low Attachment Microplates (Corning, Corning, NY) after FACS. The number of spheroids was measured 14 days after seeding. Invasion assays were performed using BD BioCoat Matrigel Matrix Cell Culture Inserts and Control Inserts (BD Biosciences, San Jose, CA) essentially as pre-

viously described.[31] Reverse transcription–polymerase chain reaction and IHC assays are described in detail in the supplementary materials (see supplementary material online at www.gastrojournal.org).

Tumorigenicity in NOD/SCID Mice

Six-week-old NOD/SCID mice (NOD/NCrCRl-*Prkdc*^{scid}) were purchased from Charles River (Charles River Laboratories, Inc, Wilmington, MA). The protocol was approved by the National Cancer Institute–Bethesda Animal Care and Use Committee. Cells were suspended in 200 μL of Dulbecco's modified Eagle medium and Matrigel (1:1), and a subcutaneous injection was performed. The size and incidence of subcutaneous tumors were recorded. For histologic evaluation, tumors were formalin-fixed, paraffin-embedded or embedded directly in OCT compound (Sakura Finetek, Torrance, CA) and stored at −80°C.

RNA Interference

A small interfering RNA (siRNA) specific to *TACSTD1* (SI03019667) and a control siRNA (1022076) were designed and synthesized by Qiagen (Qiagen, Valencia, CA). Transfection was performed using Lipofectamine 2000 (Invitrogen), according to the manufacturer's instructions. A total of 200 nmol/L of siRNA duplex was used for each transfection.

Statistical Analyses

The class comparison and gene clustering analyses were performed as previously described.[30] The canonic pathway analysis was performed using Ingenuity Pathways Analysis (v5.5; Ingenuity Systems, Redwood City, CA). The association of HCC subtypes and clinicopathologic characteristics was examined using either the Mann–Whitney *U* test or the chi-square test. Student *t* tests were used to compare various test groups assayed by colony formation, spheroid formation, or invasion assays. The Kaplan–Meier survival analysis was performed to compare patient survival or tumorigenicity.

Results

A Poor Prognostic HCC Subtype With Molecular Features of HpSC

We re-evaluated the gene expression profiles that were uniquely associated with 2 recently identified prognostic subtypes of HCC (ie, HpSC-HCC and MH-HCC), using a publicly available microarray dataset of 156 HCC cases (GEO accession number: GSE5975). Sixty cases were defined as HpSC-HCC with a poor prognosis and 96 cases were defined as MH-HCC with a good prognosis, based on EpCAM and AFP status.[27] A class-comparison analysis with univariate *t* tests and a global permutation test (1000×) yielded 793 genes that were expressed differentially between HpSC-HCC and MH-HCC ($P < .001$). Hierarchical cluster analyses revealed 2 main gene clusters that were up-regulated (cluster A; 455 genes) or down-regulated (cluster B; 338 genes) in HpSC-HCC (Figure 1*A*). Pathway analysis indicated that the enriched genes in cluster A were associated significantly with known stem cell signaling pathways such as transforming growth factor-β, Wnt/β-catenin, PI3K/Akt, and integrin ($P < .01$) (Figure 1*B*). In contrast, genes in cluster B were associated significantly with mature hepatocyte functions such as xenobiotic metabolism, complement system, and coagulation system ($P < .01$). Noticeably, known HpSC markers such as *KRT19* (CK19), *TACSTD1* (EpCAM), *AFP*, *DKK1*, *DLK1*, and *PROM1* (CD133) were up-regulated significantly in HpSC-HCC, whereas known liver maturation markers such as *UGT2B7* and *CYP3A4* were expressed more abundantly in MH-HCC (Figure 1*C* and Supplementary Tables 3 and 4; see supplementary material online at www.gastrojournal.org). Kaplan–Meier survival analysis revealed that HpSC-HCC patients had a significantly shorter survival than MH-HCC patients ($P = .036$) (Figure 1*D*). Consistently, HpSC-HCC patients had a high frequency of macroscopic and microscopic portal vein invasion (Figure 1*E*).

However, IHC analyses of an additional 79 HCC cases revealed that among 24 HpSC-HCC cases, EpCAM staining was very heterogeneous with a mixture of EpCAM$^+$ and EpCAM$^-$ tumor cells in each tumor (Figure 1*F*, *left panel*). Noticeably, many of the EpCAM$^+$ tumor cells were located at the invasion border zones and often were disseminated at the invasive front (*black arrows*). IF analysis revealed that HCC cells located at the invasive front co-expressed EpCAM, CK19, and AFP (Figure 1*F*, *right panels*). Noticeably, HpSC-HCC patients were significantly younger than MH-HCC patients (Supplementary Tables 1 and 2; see supplementary material online at www.gastrojournal.org). Enrichment of EpCAM$^+$ AFP$^+$ tumor cells at the tumor-invasive front suggested their involvement in HCC invasion and metastasis.

Isolation and Characterization of EpCAM$^+$ Cells in HCC

The results described earlier suggest that HpSC-HCC may be organized in a hierarchical fashion in which EpCAM$^+$ tumor cells act as stem-like cells with an ability to differentiate into EpCAM$^-$ tumor cells. To test this hypothesis, we first evaluated the expression pattern of 7 hepatic stem/maturation markers (EpCAM, CD133, CD90, CK19, Vimentin, Hep-Par1, and β-catenin) in 6 HCC cell lines (Figure 2*A*). All 3 AFP$^+$ cell lines (HuH1, HuH7, and Hep3B) expressed EpCAM, CD133, and cytoplasmic/nuclear β-catenin, whereas the other 3 AFP$^-$ cell lines (SK-Hep-1, HLE, and HLF) did not, consistent with the microarray data. Interestingly, AFP$^-$ cell lines had no CD90$^+$ cell population, which recently was identified as hepatic CSCs,[35] whereas AFP$^-$ cell lines had such a population. Consistent with the IF data, FACS analysis showed that AFP$^+$ cell lines had a subpopulation of

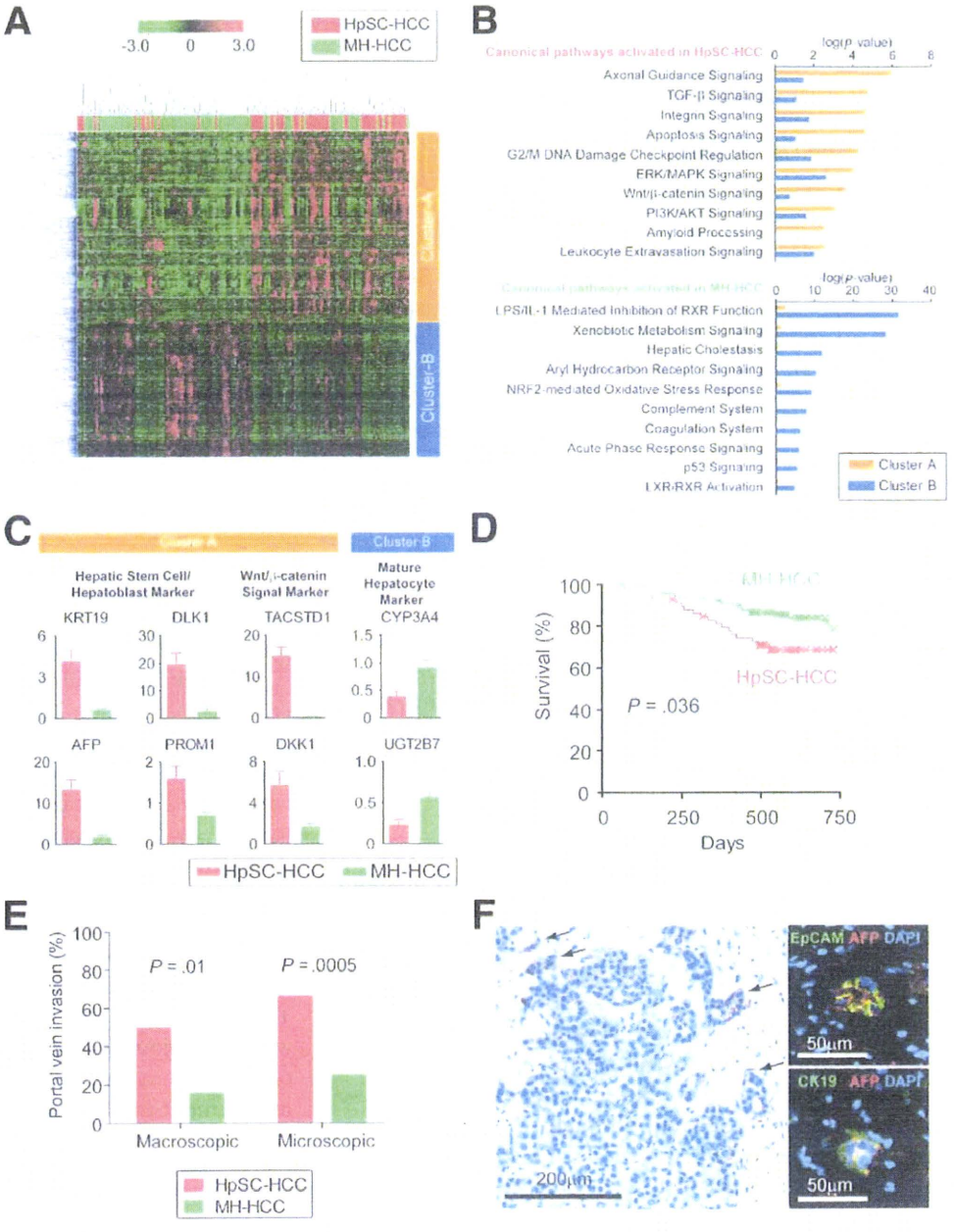

Figure 1. HpSC–HCC represents a subset of invasive HCCs with CSC features. (*A*) Hierarchical cluster analysis based on 793 HpSC–HCC–coregulated genes in 156 HCC cases. Each cell in the matrix represents the expression level of a gene in an individual sample. Red and green cells depict high and low expression levels, respectively, as indicated by the scale bar. (*B*) Pathway analysis of HpSC–HCC–coregulated genes. The top 10 canonical signaling pathways activated in cluster A (*upper panel*) or cluster B (*lower panel*) with statistical significance ($P < .01$) are shown. (*C*) Expression patterns of well-known HpSC and MH markers in each HCC subtype as analyzed by microarray. (*D*) Kaplan–Meier survival analysis of the cases used for array analysis. (*E*) Frequency of macroscopic and microscopic portal vein invasion in HpSC-HCC and MH-HCC used for IHC. (*F*) Representative images of EpCAM, AFP, and CK19 staining in HpSC–HCC samples analyzed by IHC and IF. EpCAM staining illustrates heterogeneous expression of EpCAM in HpSC-HCC (*left panel*). EpCAM$^+$ cells were disseminated in the invasive border (*left panel black arrows*) with expression of AFP (*right top panel*) and CK19 (*right bottom panel*).

EpCAM$^+$ and CD133$^+$, but no CD90$^+$ cells, whereas AFP$^-$ cell lines had a subpopulation of CD90$^+$ cells but no EpCAM$^+$ or CD133$^+$ cells (Figure 2*B*). These data indicate that HpSC-HCC and MH-HCC cell lines have distinct stem cell marker expression patterns, and EpCAM as well as CD133 may be hepatic CSC markers specifically in HpSC-HCC.

We selected 2 human HCC cell lines (HuH1 and HuH7) to isolate EpCAM$^+$ cells because both lines were heterogeneous in EpCAM, AFP, CK19, and β-catenin expression (Figure 2*A* and *B* and Supplementary Figure 1*A*; see supplementary material online at www.gastrojournal.org).[29] We successfully enriched EpCAM$^+$ and EpCAM$^-$ populations from HuH7 cells by FACS, with more than 80% purity in EpCAM$^+$ cells and more than 90% purity in EpCAM$^-$ cells 1 day after sorting (Figure 3*A*). Similar results were obtained when the purity check was performed immediately after sorting (data not shown). EpCAM$^+$ cells also were positive for CK19 and β-catenin (Figure 3*B* and Supplementary Figure 1*B*; see supplementary material online at www.gastrojournal.org) and most were AFP$^+$ (data not shown). In contrast, EpCAM$^-$ cells were negative for these markers but positive for HepPar1, a monoclonal antibody specific to hepatocytes (Figure 3*B*). Consistent with the microarray data described earlier, the levels of *TACSTD1*, *MYC*, and *hTERT* (known HpSC markers) were increased significantly in EpCAM$^+$ HuH7 cells, whereas the levels of *UGT2B7* and *CYP3A4*

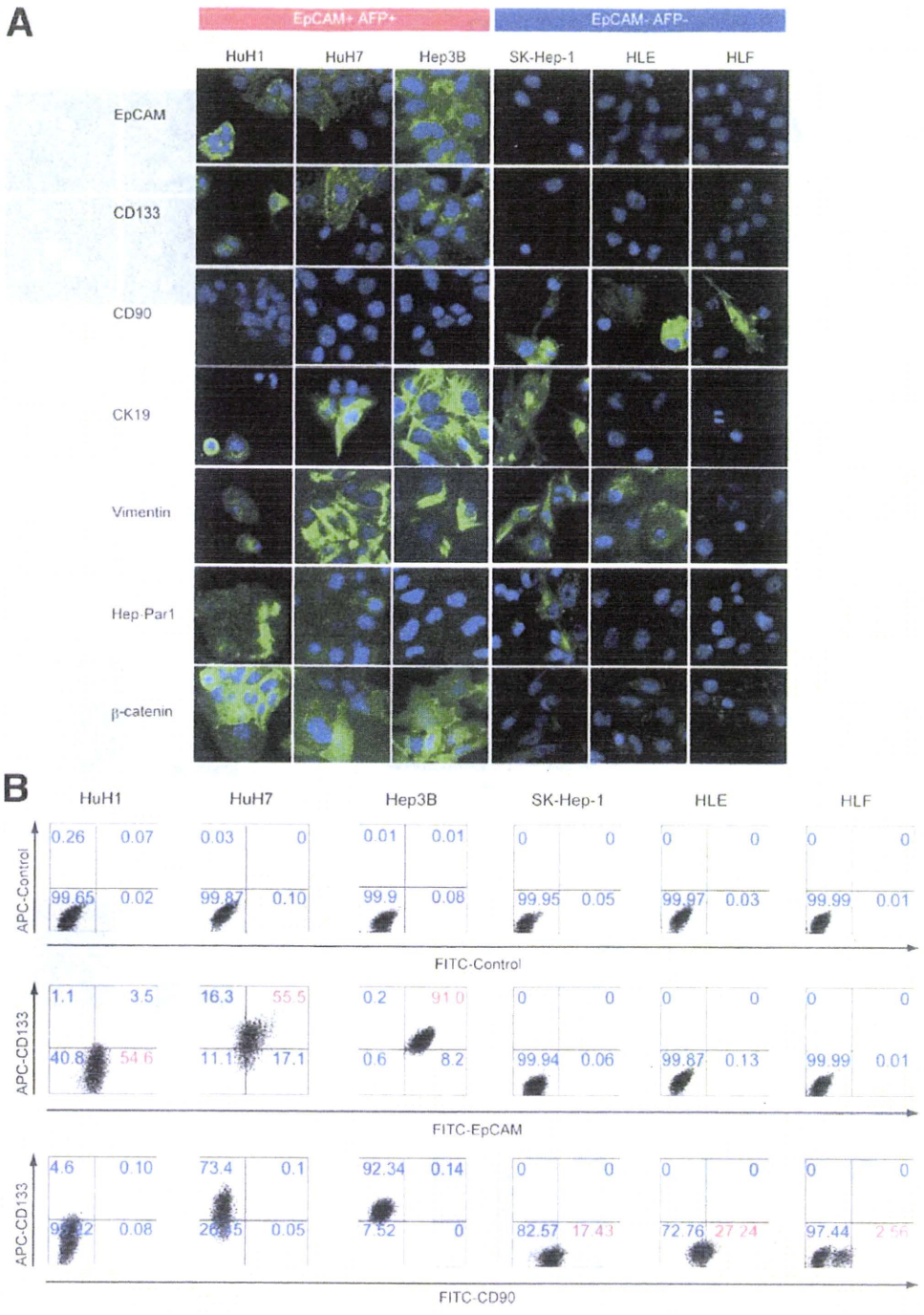

Figure 2. Characterization of hepatic stem cell marker expression in HCC cell lines. (*A*) IF analysis of 6 HCC cell lines (EpCAM$^+$ AFP$^+$ cell lines: HuH1, HuH7, and Hep3B; EpCAM$^-$ AFP$^-$ cell lines: SK-Hep-1, HLE, and HLF) stained with anti-EpCAM, anti-CD133, anti-CD90, anti-CK19, anti-Vimentin, anti–Hep-Par1, and anti–β-catenin antibodies. (*B*) FACS analysis of 6 HCC cell lines stained with anti-EpCAM, anti-CD133, and anti-CD90 antibodies.

(known mature hepatocyte markers) were significantly higher in EpCAM$^-$. HuH7 cells (Figure 3*C*, *left upper panel*). This expression pattern was reminiscent of human HpSC cells (Figure 3*C*, *left lower panel*). Similar results were obtained from HuH1 cells (data not shown). We also compared gene expression patterns of isolated HuH1, HuH7, MH, and HpSC cells using the TaqMan Human Stem Cell Pluripotency Array (Applied Biosystems, Foster City, CA) containing 96 selected human stem cell-related genes. Although a differential expression pattern of stem cell-related genes was evident among HpSC, EpCAM$^+$ HuH1, and EpCAM$^+$ HuH7 cells, the EpCAM$^+$ HCC cells were related more closely to HpSC cells whereas EpCAM$^-$ HCC cells were related more closely to diploid adult mature hepatocytes (Figure 3*C*, *right panel*; and Supplementary Figure 1*C*; see supplementary material online at www.gastrojournal.org). Thus, it appeared that EpCAM$^+$ HCC cells had a gene expression pattern that is related more closely to HpSC than EpCAM$^-$ HCC cells.

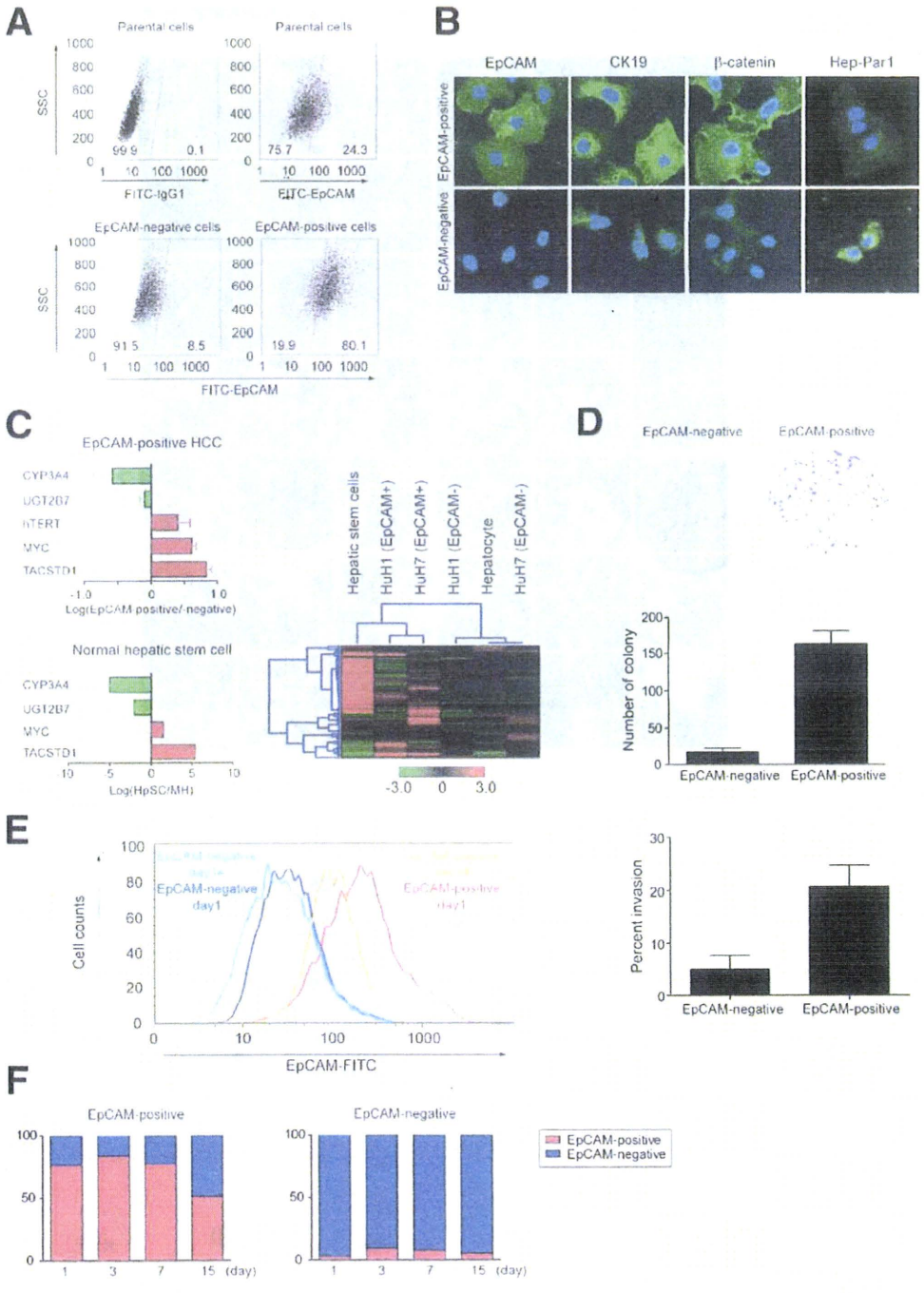

Figure 3. Characterization of EpCAM$^+$ and EpCAM$^-$ cells in HuH7 cells. (*A*) FACS analysis of EpCAM$^+$ and EpCAM$^-$ cells on day 1 after cell sorting. (*B*) IF analysis of cells stained with anti-EpCAM, anti-AFP, anti-CK19, or anti–β-catenin antibodies. (*C*) Quantitative reverse-transcription polymerase chain reaction analysis of EpCAM$^+$ and EpCAM$^-$ HuH7 cells (*left upper panel*) or HpSCs and MHs (*left lower panel*). Experiments were performed in triplicate. Hierarchical cluster analysis of HpSC, MH, and EpCAM$^+$ and EpCAM$^-$ HCC cells using a panel of genes expressed in human embryonic stem cells (*right panel*). Gene expression was measured in quadruplicate. (*D*) Representative photographs of the plates containing colonies derived from 2000 EpCAM$^+$ or EpCAM$^-$ HuH7 cells (*upper panel*). Colony formation experiments were performed in triplicate (mean ± SD) (*middle panel*). Cell invasiveness of EpCAM$^+$ and EpCAM$^-$ cells using the Matrigel invasion assay (*lower panel*). (*E*) Flow cytometer analysis of EpCAM$^+$ and EpCAM$^-$ HuH7 cells stained with anti-EpCAM at days 1 and 14 after cell sorting. (*F*) Percentage of sorted EpCAM$^+$ and EpCAM$^-$ cells after culturing for various times as analyzed by IF. Numbers of EpCAM$^+$ and EpCAM$^-$ cells were counted in 3 independent areas of chamber slides at days 1, 3, 7, and 15 after cell sorting. The average percentages of EpCAM$^+$ or EpCAM$^-$ cells are depicted as *red* or *blue*, respectively.

The isolated EpCAM$^+$ HuH7 cells formed colonies efficiently whereas EpCAM$^-$ cells failed to do so (Figure 3*D*, *upper* and *middle panels*; and Supplementary Figure 2*A* for HuH1 cells; see supplementary material online at www.gastrojournal.org). In addition, EpCAM$^+$ HuH7 cells were much more invasive than EpCAM$^-$ cells ($P < .03$) (Figure 3*D*, *lower panel*; and Supplementary Figure 2*B* for HuH1 cells; see supplementary material online at www.gastrojournal.org). The EpCAM$^+$ fraction decreased with time in sorted EpCAM$^+$ HuH7 cells from greater than 80% to 50% (Figure 3*E*). However, a small percentage of EpCAM$^+$ cells remained constant in sorted EpCAM$^-$ HuH7 cells. FACS analysis confirmed the results of IF analysis (Figure 3*F* and Supplementary Figure 2*C* for HuH7 and HuH1 cells, respectively; see supplementary material online at www.gastrojournal.org), suggesting that EpCAM$^+$ cells could differentiate into EpCAM$^-$ cells, eventually allowing an enriched EpCAM$^+$ fraction to revert back to parental cells after 14 days of culture. In contrast, EpCAM$^-$ cells maintained their EpCAM$^-$ status. In addition, we successfully isolated 12 HuH1 and 2 HuH7 colonies from 192 single-cell–plated culture wells.

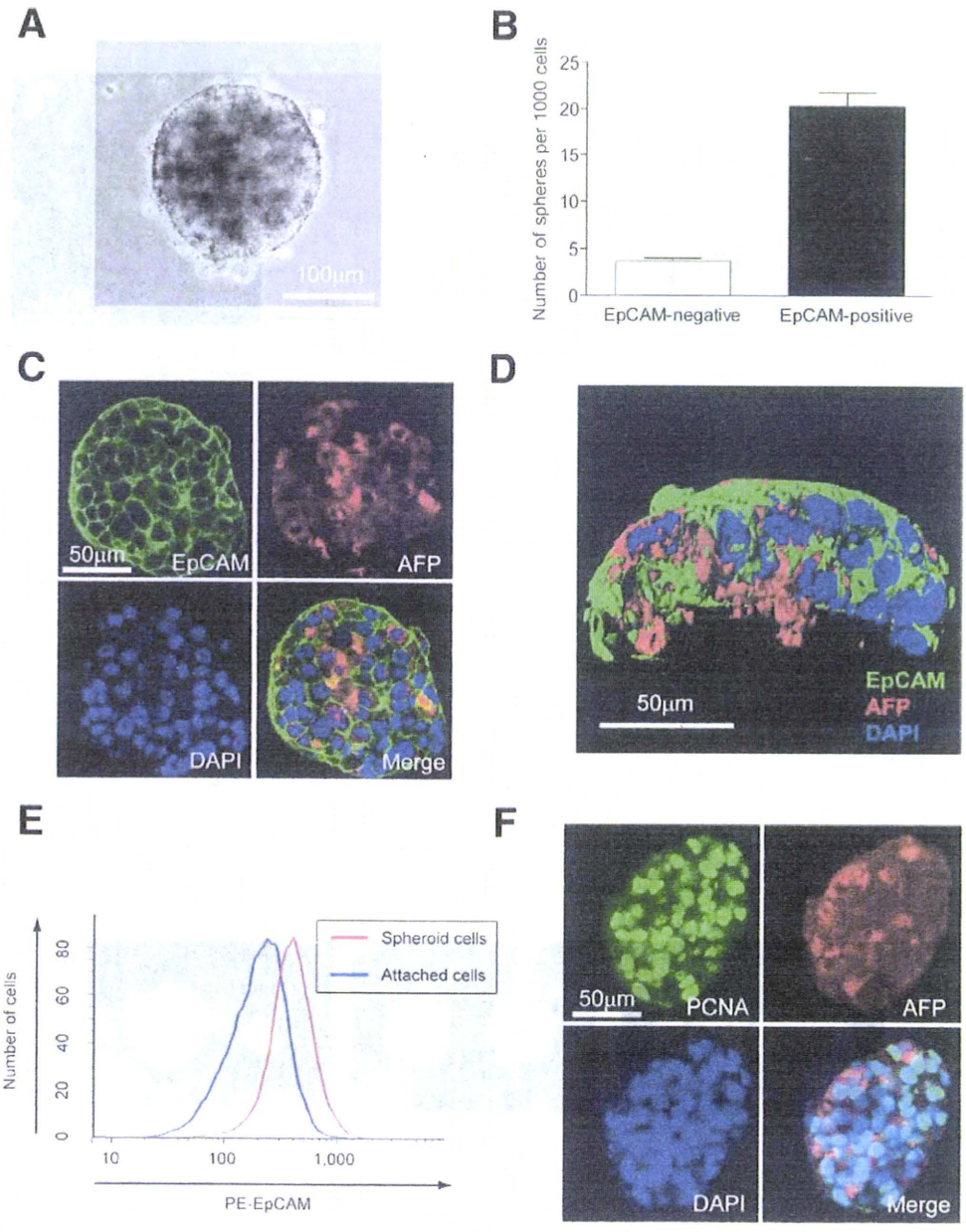

Figure 4. Spheroid formation of EpCAM$^+$ HuH1 HCC cells. (*A*) A representative phase-contrast image of an HCC spheroid derived from an EpCAM$^+$ cell (*scale bar*, 100 μm) and (*B*) total numbers of spheroids from 1000 sorted cells are shown. Experiments were performed in triplicate and data are shown as mean ± SD. (*C*) Representative confocal images of an HCC spheroid co-stained with anti-EpCAM, anti-AFP, and 4′,6-diamidino-2-phenylindole (DAPI) (*scale bar*, 50 μm). (*D*) A 3-dimensional image of an HCC spheroid co-stained with anti-EpCAM, anti-AFP, and DAPI (*scale bar*, 50 μm) reconstructed from confocal images using surface rendering. (*E*) FACS analysis of EpCAM$^+$ cells cultured as spheroid cells (*red*) or attached cells (*blue*) for 14 days after cell sorting. (*F*) Confocal images of an HCC spheroid co-stained with anti-PCNA, anti-AFP, and DAPI (*scale bar*, 50 μm).

However, all colonies were heterogeneous in EpCAM and AFP expression and no colony was completely EpCAM$^-$ (data not shown). Taken together, these results indicate that EpCAM$^+$ HCC cells resemble HpSC features. It appears that EpCAM$^+$ cells, but not EpCAM$^-$ cells, have self-renewal and differentiation capabilities with the ability to form colonies from a single cell, and produce both EpCAM$^+$ and EpCAM$^-$ cells.

It has been shown previously that stem/progenitor cells and cancer stem/progenitor cells can form spheroids in vitro in a nonattached condition.[36,37] Consistently, EpCAM$^+$ cells could form spheroids efficiently, reaching to about 150 to approximately 200 μm in diameter after 14 days of culture (Figure 4*A* and *B*). Interestingly, all cells in a spheroid were EpCAM$^+$, whereas AFP expression was relatively heterogeneous (Figure 4*C* and *D*, and Supplementary movie 1; see supplementary material online at www.gastrojournal.org). Rarely, a few spheroids derived from an EpCAM$^-$ cell fraction were positive for EpCAM (data not shown), suggesting that these spheroids were derived from contaminated residual EpCAM$^+$ cells by FACS sorting. All spheroid cells maintained EpCAM expression while half of the attached cells lost EpCAM expression when the EpCAM$^+$ fraction was cultured for 14 days (Figure 4*E*). Most spheroid cells also abundantly expressed proliferating cell nuclear antigen (PCNA), implying active cell proliferation (Figure 4*F* and Supplementary movie 2; see supplementary material online at www.gastrojournal.org). Thus, a subset of EpCAM$^+$ cells, but not EpCAM$^-$ cells, can form spheroids.

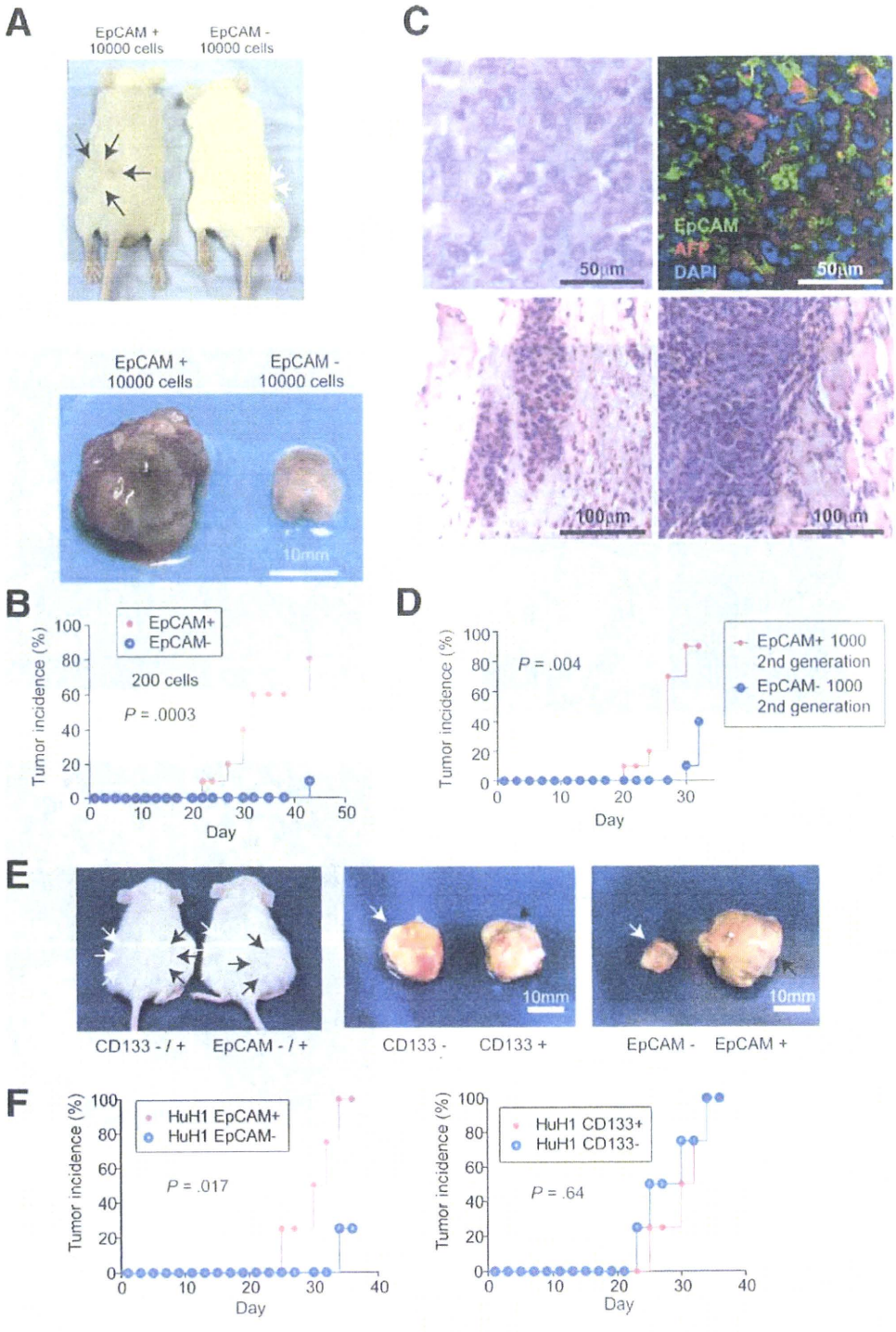

Figure 5. Tumorigenic and invasive potential of EpCAM$^+$ HCC cells. (*A*) Representative NOD/SCID mice (*upper panel*) with subcutaneous tumors (*lower panel*) from EpCAM$^+$ (*black arrows*) or EpCAM$^-$ (*white arrows*) HuH1 cells. (*B*) Tumorigenicity of 200 sorted HuH1 cells. (*C*) Histologic analysis of EpCAM$^+$ HuH1-derived xenografts. H&E staining of a subcutaneous tumor (*left upper panel*) with capsular invasion (*left lower panel*) and muscular invasion (*right lower panel*) and IF of the tumor stained with anti-EpCAM, anti-AFP, and 4′,6-diamidino-2-phenylindole (DAPI) (*right upper panel*) (*scale bar*, 50 μm). (*D*) Tumorigenicity of 1000 sorted cells derived from an EpCAM$^+$ HuH1 xenograft. Data are generated from 10 mice in each group. (*E*) Representative NOD/SCID mice (*left panel*) with subcutaneous tumors from CD133$^+$ (*black arrows*) or CD133$^-$ (*white arrows*) (*middle panel*) and EpCAM$^+$ (black arrows) or EpCAM$^-$ (*white arrows*) (*right panel*) HuH1 cells. (*F*) Tumorigenicity of 1000 HuH1 cells sorted by anti-EpCAM (*left panel*) or anti-CD133 (*right panel*) antibodies.

EpCAM$^+$ HCC Cells as Tumor-Initiating Cells

EpCAM$^+$ HCC cells, but not EpCAM$^-$ HCC cells, could efficiently initiate invasive tumors in NOD/SCID mice (Figure 5). For example, 10,000 EpCAM$^+$ HuH1 cells produced large hypervascular tumors in 100% of mice whereas EpCAM$^-$ cell fractions produced only small and pale-looking tumors in 30% of mice 4 weeks after injection (Figure 5*A* and Supplementary Figure 3*A*; see supplementary material online at www.gastrojournal.org). Similar results were obtained with HuH7 cells (Supplementary Figure 3*B–D*; see supplementary material online at www.gastrojournal.org). As little as 200 EpCAM$^+$ cells could initiate tumors in 8 of 10 injected mice, whereas 200 EpCAM$^-$ cells produced only 1 tumor among 10 injected mice at 6 weeks after transplantation, and the tumor sizes were much larger in the EpCAM$^+$ cells than in the EpCAM$^-$

cells (Figure 5*B* and Supplementary Figure 3*E*; see supplementary material online at www.gastrojournal.org). EpCAM$^+$ cells produced tumors with a mixture of both EpCAM$^+$ and EpCAM$^-$ cells in xenografts, and these cells invaded in the capsule and muscles of the leg adjacent to the tumor (Figure 5*C*). EpCAM$^+$ cells derived from tumors again maintained their tumor-initiating capacity, tumor morphology, and invasive ability in an in vivo serial transplantation experiment (Figure 5*D*). Occasionally, EpCAM$^-$ cell fractions produced a few small tumors that always contained a mixture of EpCAM$^+$ and EpCAM$^-$ cells (data not shown), indicating that the contaminated EpCAM$^+$ cells from FACS sorting contribute to the tumor-initiating ability.

To further validate whether EpCAM$^+$ HCC cells were tumor-initiating cells, we isolated EpCAM$^+$ HCC cells from 2 cases of AFP$^+$ (>600 ng/mL serum AFP) HCC clinical specimens using MACS. Consistently, 1×10^4 EpCAM$^+$ cells could induce tumors in NOD/SCID mice, but up to 1×10^6 EpCAM$^-$ cells failed to do so (Table 1). In addition, similar to HCC cell lines, fresh EpCAM$^+$ tumor cells from 2 clinical HCC specimens were more efficient in forming spheroids in vitro than EpCAM$^-$ cells (Supplementary Figure 4; see supplementary material online at www.gastrojournal.org).

FACS analysis results indicate that a majority of EpCAM$^+$ cells express CD133 in HuH7 cells but not in HuH1 cells (Figure 2*B*), which prompted us to compare the tumorigenic capacity of EpCAM$^+$ and CD133$^+$ cells in these cell lines. Noticeably, EpCAM$^+$ HuH1 cells showed marked tumor-initiating capacity compared with CD133$^+$ HuH1 cells (Figure 5*E* and *F*), whereas EpCAM$^+$ and CD133$^+$ cells had similar tumorigenic ability in HuH7 cells (data not shown).

GSK-3β Inhibition Augments EpCAM$^+$ HCC Cells

To determine the role of Wnt/β-catenin signaling[28] in EpCAM$^+$ HCC cells (Figure 1*B*), we first treated HuH1, HuH7, and HLF cells with a GSK-3β inhibitor BIO (Figure 6*A*), which activates Wnt/β-catenin signaling (Figure 6*B*) and maintains undifferentiation of embryonic stem cells.[38] 6-bromoindirubin-3′-oxime (BIO) increased the EpCAM$^+$ cell population in HuH1 and HuH7 cells when compared with the control methylated BIO (MeBIO) (Figure 6*A*). In contrast, BIO had no effect on the CD90$^+$ cell population, which is more tumorigenic than the CD90$^-$ cell population in HLF (Figure 6*A* and data not shown). Enrichment of EpCAM$^+$ cells was provoked further by the treatment of Wnt10B-conditioned media in HuH7 cells (Figure 6*C*).[34] BIO induced morphologic alteration of HuH7 cells because most cells became small and round when compared with MeBIO and suppressed EpCAM$^-$ AFP$^-$ cell populations (Figure 6*D*). Moreover, BIO induced *TACSTD1*, *MYC*, and *hTERT* expression and spheroid formation (Figure 6*E* and *F*).

Table 1. The Tumor-Initiating Capacity of EpCAM$^+$ Cells From Clinical HCC Specimens

HCC patients				Tumor incidence (mice with tumors/total no. of mice injected)	
No.	% of EpCAM$^+$ HCC cells	Groups	No. of cells injected	2 months	3 months
1	5.2	EpCAM$^+$	1×10^3	0/3	0/3
			1×10^4	2/3	2/3
			1×10^5	2/2	2/2
		EpCAM$^-$	1×10^5	0/3	0/3
			1×10^6	0/2	0/2
2	1.4	EpCAM$^+$	1×10^3	0/2	0/2
			1×10^4	0/1	1/1
		EpCAM$^-$	1×10^4	0/3	0/3
			1×10^5	0/2	0/2

EpCAM Blockage by RNA Interference

One of the hallmarks of CSCs is its resistance to conventional chemotherapeutic agents resulting in tumor relapse and thus targeting CSCs is critical to achieve successful tumor remission. Consistently, 5-FU could increase the EpCAM$^+$ population and spheroid formation of HuH1 and HuH7 cells (Figure 7*A* and *B*) (data not shown), suggesting a differential sensitivity of EpCAM$^+$ and EpCAM$^-$ HCC cells to 5-FU. In contrast, EpCAM blockage via RNA interference dramatically decreased the population of EpCAM$^+$ cells (Figure 7*C*), and significantly inhibited cellular invasion, spheroid formation, and tumorigenicity of HuH1 cells (Figure 7*D–F*). Thus, EpCAM may serve as a molecular target to eliminate HCC cells with stem/progenitor cell features.

Discussion

The cellular origin of HCC is currently in debate. In this study, we found that EpCAM can serve as a marker to enrich HCC cells with tumor-initiating ability and with some stem/progenitor cell traits. EpCAM is expressed in many human cancers with an epithelial origin.[39] During embryogenesis, EpCAM is expressed in fertilized oocytes, embryonic stem cells, and embryoid bodies, suggesting its role in early stage embryogenesis.[40] Furthermore, a recent article indicated that EpCAM is expressed in colonic and breast CSCs.[41] Taken together, these data suggest a critical role of EpCAM in CSCs as well as embryonic and somatic stem cells. Consistently, we found that EpCAM expression is regulated by Wnt/β-catenin signaling[29] and tumorigenic and highly invasive HpSC-HCC is orchestrated by a subset of cells expressing EpCAM and AFP with stem cell–like features and self-renewal and differentiation capabilities regulated by Wnt/β-catenin signaling (this study). Thus, EpCAM may be a common gene expressed in undifferentiated normal cells and HCCs with activated Wnt/β-catenin signaling. It may act as a downstream molecule

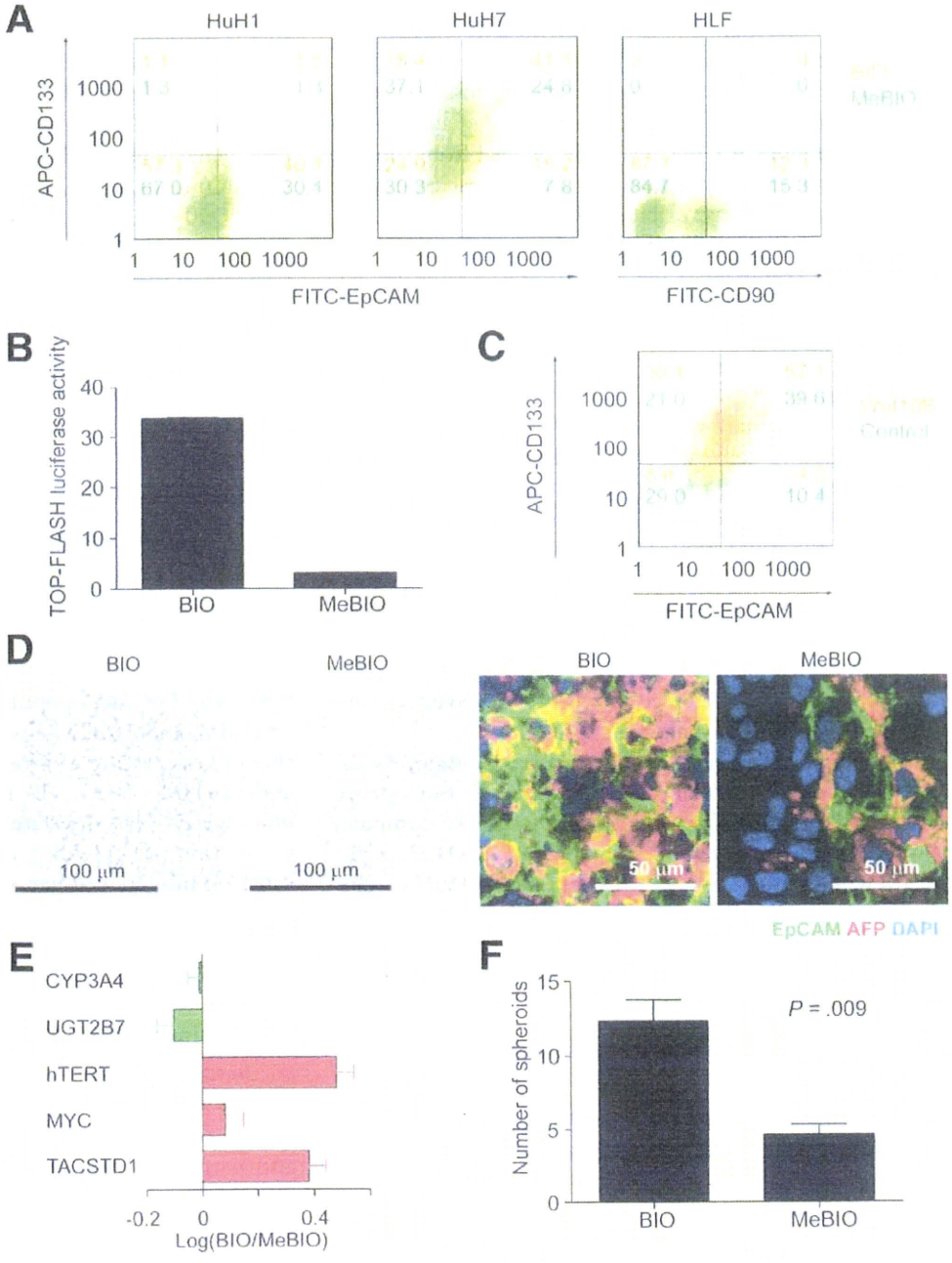

Figure 6. Wnt/β-catenin signaling augments EpCAM$^+$ HCC cells. (*A*) Flow cytometer analysis of HuH1, HuH7, and HLF cells treated with 2 μmol/L of BIO (*orange*) or MeBIO (*green*) for 10 days and stained with anti-EpCAM, anti-CD133 and anti-CD90 antibodies. (*B*) TOP-FLASH luciferase assays of HuH7 cells treated with 2 μmol/L of BIO or MeBIO. (*C*) Flow cytometer analysis of HuH7 cells cultured in normal media (Dulbecco's modified Eagle medium supplemented with 10% FBS) or Wnt10B conditioned media (details are described in the Materials and Methods section). Cells were cultured in each medium for 2 weeks. (*D*) Representative phase-contrast images (*left panel*: *scale bar*, 100 μm) or IF images (*right panel*: *scale bar*, 50 μm) of HuH7 cells treated with 2 μmol/L of BIO or MeBIO for 14 days. (*E*) Quantitative reverse transcription-polymerase chain reaction analysis of representative HpSC-HCC–related genes in HuH7 cells treated with 2 μmol/L of BIO or MeBIO for 14 days. (*F*) Spheroid formation assay of HuH7 cells treated with 2 μmol/L of BIO or MeBIO for 14 days (mean ± SD). FITC, fluorescein isothiocyanate.

to maintain HCC stemness and serve as a good marker for HCC initiating cells.

CD133 or CD90 have been used to identify potential hepatic CSCs.[35,42] CD133 is expressed in normal and malignant stem cells of the neural, hematopoietic, epithelial, hepatic, and endothelial lineages,[23,43,44] suggesting that CD133 is also a common marker to detect normal cells and CSCs. Captivatingly, EpCAM expression overlaps with CD133 expression in normal human colon tissues and colorectal cancer tissues, yet CD133$^+$ and CD133$^-$ cells are equally tumorigenic.[45] Similarly, we found that EpCAM$^+$ and EpCAM$^-$ HuH1 cells equally expressed CD133, but only EpCAM$^+$ cells developed large hypervascular tumors. Our data suggest that EpCAM may be a better marker than CD133 to enrich HCC tumor-initiating cells from AFP$^+$ tumors. We also found that CD90 expression was limited to HCC cell lines that are EpCAM$^-$ AFP$^-$, and Wnt/β-catenin signaling had little effect on CD90$^+$ cell enrichment. These results suggest that the expression patterns of various stem cell markers in tumor-initiating cells with stem/progenitor cell features may be different in each HCC subtype, possibly owing to the heterogeneity of activated signaling pathways in normal stem/progenitor cells where these tumor-initiating cells may originate. Therefore, it would be useful to

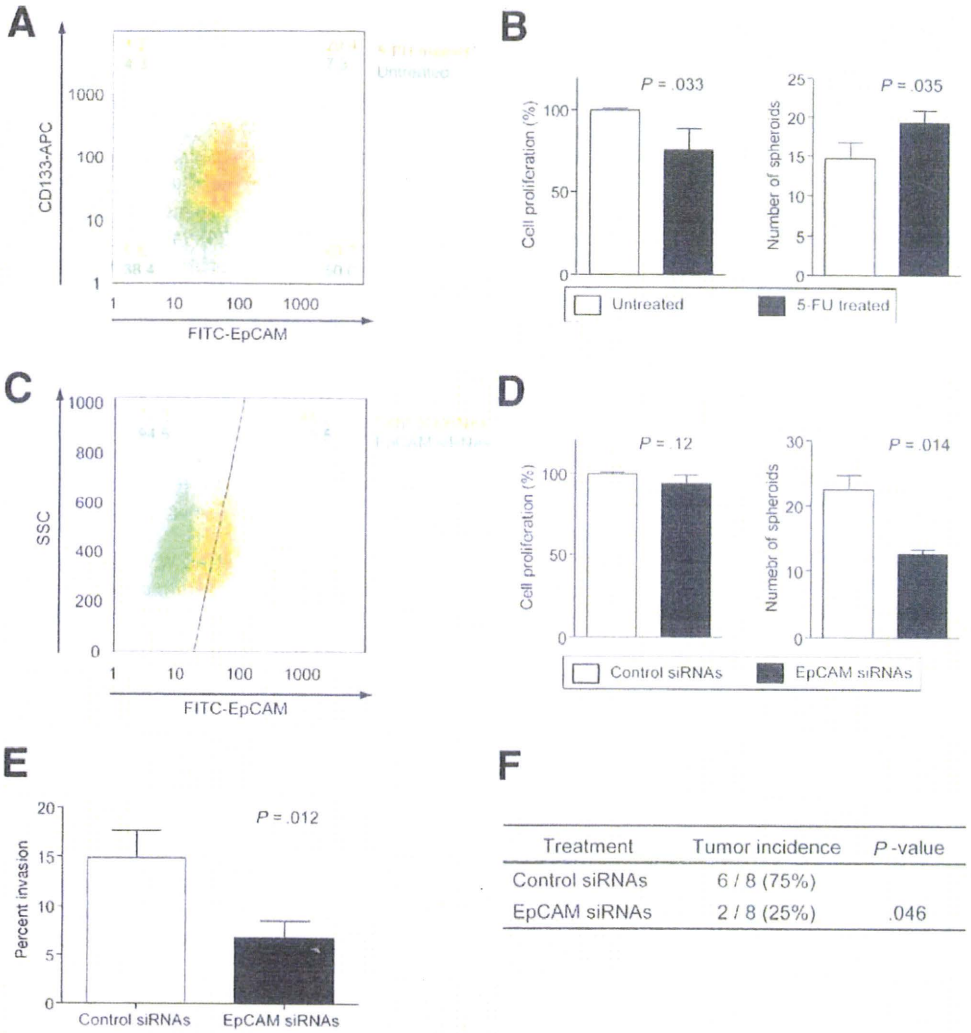

F

Treatment	Tumor incidence	*P*-value
Control siRNAs	6 / 8 (75%)	
EpCAM siRNAs	2 / 8 (25%)	.046

Figure 7. EpCAM blockage inhibits the tumorigenic and invasive capacity of EpCAM$^+$ HCC cells. (*A*) Enrichment of EpCAM$^+$ cells after 5-FU treatment. HuH1 cells refer as control or without treatment (*green*) or treated with 2 μg/mL of 5-FU (*orange*) for 3 days and analyzed by FACS using anti-EpCAM and anti-CD133 antibodies. (*B*) Spheroid formation of HuH1 cells treated with 2 μg/mL of 5-FU for 3 days. (*C*) FACS analysis of HuH1 cells treated with a control siRNA (orange) or EpCAM-specific siRNA (*green*) at day 3 after transfection. (*D*) Spheroid formation or (*E*) invasive capacity ofEpCAM$^+$ HuH1 cells transfected with a control siRNA or EpCAM-specific siRNA. Experiments were performed in triplicate and the data are shown as mean ± SD. (*D*) siRNAs. (*F*) Inhibition of tumor formation in vivo by EpCAM gene silencing. EpCAM$^+$ HuH1 cells were transfected with siRNA oligos and 1000 cells were injected 24 hours after transfection.

comprehensively investigate the expression patterns of stem cell markers to characterize the population of CSCs that may correlate with the activation of their distinct molecular pathways.

CSCs may be more resistant to chemotherapeutic agents than differentiated tumor cells possibly owing to an increased expression of adenosine triphosphate–binding cassette transporters and anti-apoptotic proteins.[4] Thus, the development of an effective strategy to target CSC pools together with conventional chemotherapies is essential to eradicate a tumor mass.[14] By blocking the programs that activate self-renewal and/or inhibit asymmetric division, CSC features could be destemmed.[46,47] Consistently, EpCAM blockage could inhibit cellular invasion and tumorigenicity of EpCAM$^+$ HCC cells, revealing the feasibility of targeting a CSC marker to destem CSC features. EpCAM may induce c-Myc,[48] a common molecular node activated in HpSC-HCC.[27] c-Myc, together with Oct3/4, Sox2, and Klf4, can induce pluripotent stem cells from adult fibroblasts.[49] It is possible that EpCAM blockage to inhibit hepatic CSCs may result in a suppression of c-Myc signaling. Encouragingly, EpCAM-specific antibodies are currently in phase II clinical trials.[50] Furthermore, a recent study indicated that EpCAM$^+$ circulating tumor cells identified by a unique microfluidic platform can be used to monitor outcomes of patients undergoing systemic treatment.[51] Therefore, it may be useful to combine EpCAM antibodies with conventional chemotherapy to target both CSCs and non-CSCs for the treatment of HCC.

Supplementary Data

Note: To access the supplementary material accompanying this article, visit the online version of *Gastroenterology* at www.gastrojournal.org, and at doi: 10.1053/j.gastro.2008.12.004.

References

1. Fialkow PJ. Clonal origin of human tumors. Biochim Biophys Acta 1976;458:283–321.